Gaona Cordero, A.; Díaz Morales, UM.; Corma Canós, A. (2017). Functional Acid and Base Hybrid Catalysts Organized by Associated (Organo)aluminosilicate Layers for C-C Bond Forming Reactions and Tandem Processes. Chemistry of Materials. 29(4):1599-1612. doi:10.1021/acs.chemmater.6b04563

Functional acid and base hybrid catalysts organized by associated (organo)aluminosilicate layers for C-C bond forming reactions and tandem processes

Aidé Gaona, Urbano Díaz*, Avelino Corma*

Instituto de Tecnología Química, Universitat Politècnica de València-Consejo Superior de Investigaciones Científicas, Avenida de los Naranjos s/n, E-46022 Valencia, Spain
Tel.: +34963877800 FAX: +34963877809 E-mail: udiaz@itq.upv.es; acorma@itq.upv.es

Abstract

Novel bifunctional acid-base monolayered hybrid catalysts (MLHMs), based on associated individual (organo)aluminosilicate sheets with amino and sulfonic pending groups located in the interlayer space, have been successfully prepared by direct alkaline hydrothermal synthesis and evaluated in consecutive catalytic transformations. Different characterization techniques such as chemical and thermogravimetrical analyses, X-ray diffraction, TEM microscopy, nuclear magnetic resonance (NMR), temperature programmed desorption of CO_2 and NH_3 (TPD), and textural measurements were used to show physico-chemical and structural nature of the materials, evidencing their effectivity as functional acid, base and acid-base catalysts for different one-pot two-step tandem reactions, which were performed in presence of only one active and recoverable lamellar-type hybrid solid catalyst.

Introduction

The capacity to keep the high reactivity of soluble organocatalysts, being reused during successive reaction cycles, has been achieved through the structural inclusion of modified organic functions or precursors in specific positions of stable and robust inorganic porous networks.[1, 2] This goal has partially been achieved in the last decade with the generation of novel families of organic-inorganic hybrid materials that contain different active functions in their frameworks, being developed authentic multi-functional hybrid catalysts.[3] The possibility to isolate and heterogenize, into the inorganic matrixes, chiral, base, acid and/or redox centers, separated at controlled molecular distances, to perform in one-pot consecutive or cascade reactions is still in clear growth in materials science field.[4-6] Important advances has recently been carried out with the preparation of novel multi-functional organosiliceous materials or metalorganic structures capable to perform multi-component chiral reactions or multi-step processes catalyzed by only one recoverable hybrid solid catalyst in one-pot catalytic pathway.[7] However, in the majority of the cases, long reaction times, associated leaching phenomenon and low yield and stereoselectivity are observed. The random distribution of the different heterogenized organic functions, together with the intrinsic inorganic active sites present in the framework, would be the main reason to explain the reactivity and selectivity decrease, more often detected when multi-functional hybrid materials are used as catalysts for cascade or consecutive reactions.[8, 9]

This important drawback should be mitigated through two possible approaches: (i) design and preparation of specific organic-inorganic precursors where the different functions will be pre-located and pre-stabilized before their incorporation into the porous network,[2] and (ii) use of optimized syntheses processes that allow controlling the final location of active functions in the structure.[10]

Taking in account the first approach, sophisticated and costly organosilanes, bridged silsesquioxanes or specific organic linkers have been prepared to obtain multi-functional organosilicon mesoporous materials,[11] organozeolites,[12] metalorganic frameworks[13] and coordination polymers.[14] It is the case of the urea based-cinchona silyl derivatives, used to generate novel families of multi-site chiral mesoporous organosilica materials, active to promote asymmetric multi-component reactions.[15] In addition, the preparation of periodic mesoporous organosilicas (PMOs) based on chiral BINAP or quinuclidine silyl active builder units are examples of efficient hybrid catalysts structured from specific silsesquioxanes or disilane precursors, with different functions located in their organic bridges between terminal siloxane groups.[16]

Another approach to prepare multi-functional organic-inorganic materials, controlling the specific position where active sites are situated in the network, come from the use of suitable synthesis' methodologies.[17] In fact, optimized sol-gel,[18] micellar,[19] solvothermal[20] or hydrothermal

routes[21] have been used to synthesize hybrid materials through the *in-situ* formation and assembly of individual structural builders, such as metallic clusters or nodes,[22] organometallic complexes,[23] organosilicon tetrahedron,[24] organic linkers or ligands[25] and nanosheets,[26, 27] among the most habitual in hybrid materials. However, in most cases, only one active site is finally located into the framework accessible to reactants, being frequently necessary additional post-synthesis treatments to incorporate further functions in the hybrid materials in specific positions.[28, 29] Successive anchoring or tethering processes in delaminated zeolites or metalorganic frameworks (MOFs), as well as long swelling and pillarization processes carried out on previously synthesized lamellar precursors confirm this fact.[30, 31]

Recently, optimized solvothermal and hydrothermal synthesis processes in presence of specific organic dual templates or linkers have allowed the direct preparation, in only one-step synthesis process, of individual zeolitic or metalorganic nanosheets capable to lodge different active functions into their framework.[32] In this latter case, the organic templates or linkers should act as structure directing agents and as 3D growth inhibitors, providing additional active functions to final formed hybrid nanolayers.[33] Also, in the last years, hydrothermal synthesis routes in presence of active bridged silsesquioxanes and aluminum-rich alkaline media have allowed the direct preparation of novel families of layered hybrid materials (ECS and LHM type solids), in only one synthesis step, based on inorganic layers covalently connected through organic active pillars placed in the interlayer region to generate catalysts useful for C-C bond forming processes.[34, 35]

Taking this into account, we have now prepared functional acid-base hybrid materials (MHLMs) based on associated individual (organo)aluminosilicate layers through direct hydrothermal synthesis processes in presence of aluminum-rich alkaline media and two combined types of organosiloxane precursors. The result has been the formation of isolated aluminosilicate sheets with amino and/or sulfonic groups homogeneously distributed along their external surface, located between the individual layers. The polar interaction between the individual hybrid nanolayers, through pending groups, facilitates the association of them to generate stable and ordered like lamellar hybrid materials. The solids were characterized through different suitable characterization techniques such as chemical and thermogravimetrical analyses, X-ray diffraction, TEM microscopy, nuclear magnetic resonance (NMR), temperature programmed desorption of CO_2 and NH_3 (TPD), and textural measurements, being effective as functional acid, base and acid-base catalysts for different one-pot two-step tandem reactions based on C-C bond forming processes, performed in presence of only one active and recoverable lamellar-type hybrid solid catalyst.

Experimental

Reagents

Monolayered hybrid materials (MLHM) were synthesized using triethoxymethylsilane (TEMS, Aldrich), (3-aminopropyl)trimethoxysilane (APTMS, Aldrich) and (3-mercaptopropyl)trimethoxysilane (MPTMS, Aldrich) as silica sources (Figure 1a). Sodium aluminate ($NaAlO_2$, Carlo Erba/ Riedel Haen) and NaOH (Aldrich) were used as aluminum and alkaline reagents, respectively. Acid ethanolic solution (0.02 M H_2SO_4) was used for oxidation post-synthesis processes. Dodecyltrimethylammonium bromide (C_{12}TMABr, Aldrich), cetyltrimethylammonium hydroxide (C_{16}TMAOH, Aldrich) and octadecyltrimethylammonium bromide (C_{18}TMABr, Aldrich) were used as swelling agents.

Synthesis of Monolayered Hybrid Materials (MLHM)

x-MLHM-NH_2 and x-MLHM-NH_3^+

The synthesis gel was prepared by addition of organosilicon, TEMS and APTMS, precursors to an aqueous solution of sodium aluminate ($NaAlO_2$) and NaOH, achieving the following molar ratios: Si/Al=1.02, Na/Si=1.28, NaOH/Si=0.18 and H_2O/Si=13. Samples were prepared using different (1-x)TEMS:(x)APTMS mole fractions. Specifically, 1:0 (100-MLHM-TEMS), 0.95:0.05 (5-MLHM-NH_2), 0.85:0.15 (15-MLHM-NH_2), 0.7:0.3 (30-MLHM-NH_2), 0.5:0.5 (50-MLHM-NH_2) and 0:1 (100-MLHM-NH_2) based on Si contribution were considered.

The resulting slurry was homogenized through continuous stirring at room temperature until gelification, which depends on the different percentage of organosilicon precursors in the mixture. Then, it was introduced into a stainless steel autoclave and heated at 135 ºC for 9 days under autogenous pressure and static conditions. After cooling up to room temperature, the solid was isolated, washed with distilled water and dried overnight at 60 ºC, obtaining the samples named x-MLHM-NH_2.

x-MLHM-NH_3^+ samples were obtained from x-MLHM-NH_2 materials by stirring with acid ethanolic solution (0.02 M H_2SO_4) for 24 h at room temperature. Thus, x-MLHM-NH_2 samples were protonated (amino groups) with the objective to study the influence of formed ammonium groups in their performance as base catalyst. Protonated-amino hybrid materials were recovered, filtrated, washed with ethanol and dried overnight at 60 ºC.

x-MLHM-SH and x-MLHM-SO_3H

The followed methodology to obtain x-MLHM-SH was the same above described for x-MLHM-NH_2, except that in this case, a mixture of TEMS and MPTMS was used as organosilicon precursors. Samples were prepared with different (1-x)TEMS:(x)MPTMS mole fractions. Specifically,

0.95:0.05 (5-MLHM-SH), 0.85:0.15 (15-MLHM-SH), 0.7:0.3 (30-MLHM-SH), 0.5:0.5 (50-MLHM-SH) and 0:1 (100-MLHM-SH) based on Si contribution were considered. When x=0.3 and x=0.5, crystallization needed higher temperatures and hydrothermal synthesis process was carried out at 150 ºC for 9 days under static conditions.

In order to transform thiol groups in sulfonic acids, the solid hybrids were stirred with acid ethanolic solution (0.02 M H_2SO_4) for 24 h at room temperature. The solid products obtained were isolated, washed with ethanol and dried overnight at 60 ºC, obtaining the samples named x-MLHM-SO_3H.

x-MLHM-NH_2-SH and x-MLHM-NH_2-SO_3H

Similar synthesis methodology was performed to obtain the hybrid materials x-MLHM-NH_2-SH. However, in this case, a mixture of TEMS, APTMS and MPTMS was used as silicon source. Samples were prepared with different (1-2x)TEMS:(x)APTMS:(x)MPTMS mole fractions. Specifically, 0.7:0.15:0.15 (15-MLHM-NH_2-SH), 0.4:0.3:0.3 (30-MLHM-NH_2-SH), 0:0.5:0.5 (50-MLHM-NH_2-SH) based on Si contribution were considered. The acid oxidation post-synthesis processes to obtain amino-sulfonic-bifunctional hybrid material (x-MLHM-NH_2-SO_3H) was the same above described.

Characterization Techniques

XRD analysis was carried out with a Philips X'PERT diffractometer equipped with a proportional detector and a secondary graphite monochromator. Data were collected stepwise over the $2º \leq 2\theta \leq 20º$ angular region, with steps of 0.02º 2θ, 20s/step accumulation time and Cu$K\alpha$ (λ=1.54178 Å) radiation. Transmission electron microscopy (TEM) micrographs were obtained with a JEOL JEM2100F electron microscope operating at 200 keV. The samples were prepared directly by dispersing the powders onto carbon copper grids. C, N, S and H contents were determined with a Carlo Erba 1106 elemental analyser, while Si, Al and Na contents were obtained by means of atomic absorption spectroscopy (Spectra AA 10 Plus, Varian). Thermogravimetric and differential thermal analyses (TGA-DTA) were conducted in an air stream with a Metler Toledo TGA/SDTA 851E analyser.

Nitrogen adsorption isotherms were measured at -196 ºC with a Micromeritics ASAP 2010 volumetric adsorption analyser. Before the measurements, the samples were outgassed for 12 h at 100 ºC. The BET specific surface area[36] was calculated from the nitrogen adsorption data in the relative pressure range from 0.04 to 0.2. The total pore volume[37] was obtained from the amount of N_2 adsorbed at a relative pressure of about 0.99. External surface area and micropore volume were estimated using the *t*-plot method in the *t* range from 3.5 to 5. The pore diameter and the pore size

distribution were calculated using the Barret-Joyner-Halenda (BJH)[38] method on the adsorption branch of the nitrogen isotherms.

Basic sites were determined by means of CO_2-TPD in an Autochem II chemisorption analyser connected to a Thermostar mass spectometer. Before exposure to CO_2, all the samples (0.1 g) were pre-treated in situ at 100ºC in a He flow for 2.5 h. Then, the temperature was lowered to room temperature and the sample was saturated with pulses of CO_2 for 1 h. Afterward, CO_2 desorption began with a heating rate of 10ºC/min up to 800ºC.

The acidity of the catalysts was measured by NH_3-TPD. The analysis was performed with an Autochem II chemisorption analyser. The samples (0.1 g) were pre-treated in an Ar flow at 100ºC for 60 min, equilibrated to 100ºC in an He flow, and saturated with pulses of NH_3 in He. Desorption was performed by heating the sample at 10ºC/min from 100ºC to 800ºC. The TPD profiles of the catalysts were recorded with a TCD detector and the compounds desorbed were identified with a Thermostar mass spectrometer.

Solid state MAS-NMR spectra were recorded at room temperature under magic angle spinning (MAS) in a Bruker AV-400 spectrometer. The single pulse ^{29}Si spectra were acquired at 79.5 MHz with a 7 mm Bruker BL-7 probe, using pulses of 3.5 μs corresponding to a flip angle of 3/4 π radians, and a recycle delay of 240 s. The ^{1}H to ^{13}C cross-polarization (CP) spectra were acquired by using a 90° pulse for ^{1}H of 5 μs, a contact time of 5 ms and a recycle of 3 ms. The ^{13}C spectra were recorded with a 7 mm Bruker BL-7 probe and at a sample spinning rate of 5 kHz. ^{13}C and ^{29}Si were referred to adamantine and tetramethylsilane, respectively.

Liquid state ^{13}C NMR spectra were recorded at 75 MHz using a Bruker AMX300 instrument, whilst ^{29}Si NMR spectra were recorded at 60 MHz. Chemical shifts are quoted in ppm and are referenced to the appropriate residual solvent peak.

Catalytic tests

Catalyst tests were carried out in a closed conic vessel under nitrogen atmosphere and continuous magnetic stirring.

Base catalysis

Knoevenagel condensations

- *Ethyl 2-benzylideneacetoacetate*: A mixture of benzaldehyde (2.0 mmol) and ethyl acetoacetate (2.0 mmol) at 80 ºC, under an inert atmosphere (N_2), was magnetically stirred, and 10 mol% of N, present in the solid catalyst, were added. 1 mL of acetonitrile was used as solvent.

- *Diethyl 2-benzylidenemalonate:* A mixture of benzaldehyde (2.0 mmol) and diethylmalonate (1.74 mmol) at 110 ºC, under an inert atmosphere (N_2), was magnetically stirred, and 10 mol% of N, present in the solid catalyst, were added. 1 mL of toluene was used as solvent.

Henry reaction

- *Nitrostyrene:* A mixture of benzaldehyde (2.0 mmol) and nitromethane (8.0 mmol) at 90 ºC, under an inert atmosphere (N_2), was magnetically stirred, and 5 mol% of N, present in the solid catalyst, were added. 1 mL of anisole was used as solvent.

Acid catalysis

- *Acetalization of benzaldehyde with methanol:* A mixture of benzaldehyde (0.94 mmol) and methanol (3 mL) at 45 ºC, under an inert atmosphere (N_2), was magnetically stirred, and 10 mol% of S, present in the solid catalyst, were added.

One-pot tandem cascade reaction

Deacetalization-Knoevenagel reaction

A mixture of benzaldehyde dimethylacetal (2.17 mmol), ethyl cyanoacetate (2.01 mmol) and H_2O (18µL) at 90 ºC, under an inert atmosphere (N_2), was magnetically stirred, and 5 mol% of N, present in the solid catalyst, were added. 1 mL of acetonitrile was used as solvent.

In the catalytic tests, the reaction was monitored by taking periodically samples, the evolution, being followed by Gas Chromatography (GC) equipped with a HP-5 column (30m x 0.25mm x 0.25µm) or HP innowax column (60m x 0.32mm x 0.25µm) and a FID as detector. When samples were analyzed by the GC, the quantification of the reaction components was done by relating the peak surface areas to known concentrations for each component. Thus, the values of the areas for each component were represented versus the concentration, obtaining a straight line Area= f(Concentration). From these calibration curves, it was possible to calculate the concentration for the samples taken in the catalytic experiments. Therefore, from GC data and calibration curves, conversions (*%X*), yields (*Y%*) and selectivities (*%S*) values were established:

$$X(\%) = \left(\frac{[Reactant]_{t=0} - [Reactant]_{t=t}}{[Reactant]_{t=0}}\right) \times 100$$

$$Y(\%) = \left(\frac{[Product]_{t=t}}{[Reactant]_{t=0}}\right) \times 100$$

$$S(\%) = \left(\frac{Y(\%)}{X(\%)}\right) \times 100$$

Furthermore, no pre-treatments were performed with the solid catalysts before catalytic tests. When catalyst reuses were carried out, the solid was filtered and thoroughly washed with ethanol after each run and then dried at 60ºC for 12 h.

Results and Discussion

Synthesis and characterization

Usually, synthesis slurries preparation in alkaline media with high aluminum presence together with the use of silicon precursors containing reactive terminal siloxane groups, facilitates the production of stable microporous silica-aluminas with low Si/Al molar ratios.[39] This fact was also detected in the lamellar materials here studied, which were formed by ordered organic silicoaluminate monosheets with methyl, amino and/or thiol-sulfonic pending organic moieties. The favorable polar interaction established between individual organic-inorganic monosheets facilitated the formation of lamellar structures based on perpendicularly aligned organic silicoaluminate layers associated through weak chemical bonding, such as Van der Waals, hydrogen bonding or ionic interactions (Figure 1b). It is remarkably that the crystallization was attained without using structural directing agents (SDA's) in only one hydrothermal synthesis step.

The XRD patterns of the as-synthesized samples (x-MLHM-NH_2, x-MLHM-SH and x-MLHM-NH_2-SH) showed the presence of first *(100)* diffraction band, own of conventional ordered layered materials, being possible to precisely calculate the basal space present in the solids (Figure S1, S2 and Figure 2). Specifically, the monolayered hybrid material obtained in unique presence of TEMS (100-MLHM-TEMS) showed a main basal space of 8.7 Å, which agrees with the presence of attached methyl groups with 2.5 Å of length, located between two contiguous nanosheets whose thickness would be approximately 5.4 Å. This data would be in consonance with similar thicknesses exhibited by inorganic layers, such as makatite-type, which are the base of well-known inorganic lamellar silicates as magadiite or kenyaite[40, 41] and silicoaluminates prepared from synthesis gels with high aluminum presence.[42] So, these thin monolayers detected in the materials here considered, would be structured by strong covalent connection between organosilicon and aluminum tetrahedra, generating intralayer six member rings (6MR) which would be located along the plane *bc* of the organic-inorganic sheets, such as it was previously described for ECS and LHM-type[34, 35] materials.

The solids obtained using propylamine precursor (x-MLHM-NH_2) exhibited diffraction patterns with a progressive increase in the basal distance towards lower 2θ angles due to the larger molecular length of the APTMS (Figure S1). When the hybrid material was synthesized with 100% APTMS as silicon source (100-MLHM-NH_2, Figure S1f), the diffraction pattern showed that the organic-inorganic sheets were separated by ~10.2 Å. Therefore, if it is assumed that the inorganic layers' thickness is around 5.4 Å and considering that the molecular length of the pending amino groups from APTMS is ~ 6.1 Å, it can be deduced that a slight flexion of aminogroups has taken place in the interlayer space, which possibly is due to attractive weak interactions among two consecutive monolayers, due to presence of polar pending groups.

Similar tendencies to lower 2θ angles were observed in the diffractograms when mol fraction of MPTMS was increased during the synthesis (x-MLHM-MPTMS), compared with basal space observed for 100-MLHM-TEMS material (Figure S2). In the case that only MPTMS was used as silicon precursor, basal space increased until ~ 13.6 Å (Figure S2f). Hence, considering the thickness of nanosheets (5.4 Å), the interlamellar space occupied by propylthiol groups from monosilane precursor correspond to 8.2 Å, which is close to the molecular length of the organic fragment. However, the exact molecular length of the MPTMS is 6.5 Å, and probably inherent versatility of lamellar materials together with the presence of interlamellar solvent molecules could be the reason of a larger separation between individual layers. Similarity, the diffractograms of x-MLHM-NH_2-SH materials exhibited an increase of *(100)* basal space, when the presence of amino and thiol organic fragments was rising in the synthesis gel, up to ~ 13.0 Å for 50-MLHM-NH_2-SH material (Figure 2). In general, the results would imply the existence of ordered organic silicoaluminate sheets, placed perpendicularly to axis *a* and separated by homogeneously distributed pending organic moieties from monosilanes used as organosilicon monomer precursors, which are situated in the interlayer region.

When oxidation post-synthesis process was carried out in order to convert thiol groups in sulfonic acidic moieties for x-MLHM-SH and x-MLHM-NH_2-SH samples (named x-MLHM-SO_3H and x-MLHM-NH_2-SO_3H), the diffraction patterns of the samples obtained (Figure S3 and Figure S4) were similar to as-made samples. Thus, acid process produced neither a marked shifting nor a decrease in the intensity of the *(100)* diffraction band, indicating that the lamellar organization and structuration are preserved after the oxidation of the thiol groups. However, oxidized samples showed a slight higher basal space, since molecular length for sulfonic acid is a little larger than thiol monosilane (Figure 1a).

It is important to point out that, in all diffractograms, it is observed (*0kl*) diffraction bands at higher 2θ angles than 12º that are not entailed to the lamellar order, this fact being detected in this type of hybrid materials. This result shows that the utilization of several organosilicon precursors or their combined use facilitates the crystallization of (organo)aluminosilicate layers with similar thicknesses and structure, and only slight modifications occurs during the hydrothermal alkaline synthesis. These common bands confirm that the structural integrity of MLHM materials was preserved despite wide variety of compositions used in the synthesis slurry and the performed post-synthesis oxidation processes. However, the low intensity of *(0kl)* diffraction peaks, associated to the network of the individual layers in the *bc* plane*,* especially when thiol/sulfonic groups were involved, would be illustrative of the low crystallinity attained in this type of organic silicoaluminate sheets, being this also detected in standard lamellar silicates, such as magadiite, kenyaite or illerite[43], or in previously described ECS and LHM-type silicoaluminates. [35, 44]

The layered organization of the hybrid solids here prepared was also analyzed and corroborated by means of swelling with surfactants of different molecular length, such as C_{12}TMABr, C_{16}TMAOH and C_{18}TMABr (Figure 1c), being possible to confirm this morphological spatial swelled organization by XRD. Figure S5 shows several swollen MLHM-type materials from above mentioned swelling agents, being detected that when molecular length of the surfactants increased, *(100)* basal space showed by swollen materials also was consequently higher.

Transmission electronic microscopy (TEM) was used to visualize the lamellar morphology of the MLHM monolayered hybrid materials (Figure 3). The hybrid materials synthesized in presence of only TEMS (100-MLHM-TEMS) were composed of nanosheets forming a plate-like hierarchical structure (Figure 3a), characteristic of conventional lamellar materials, such as layered double hydroxides (LDHs)[45] or lamellar zeolitic precursors[46], the detected layered stacking being different in each crystal. Specifically, single organo silicoaluminate sheets were identified and the interlayer distance between two consecutive organic-inorganic nanosheets, separated by organic pending moieties, was observed (Figure 3b). When thiol and/or amino groups were involved in the synthesis, hybrids materials were also formed by individual crystals with similar plate-type morphology (Figure 3c-f and Figure S6).

The composition of the different as-made monolayered hybrid materials (MLHM) was followed by means of chemical analysis (Tables S1, S2 and S3). The results obtained show that organic fragments were present in the solid hybrids obtained from organosiloxane monomers. Specifically, in the solids prepared using APTMS and TEMS as organosilane precursors, x-MLHM-NH_2 (Table S1), when the amount of moles from APTMS was increasing during the synthesis process respect total SiO_2 moles, the nitrogen content was also increased. Therefore, the nitrogen content obtained in each sample would be indicative of the incorporation of amino-silyl groups forming the structure of the materials, even if APTMS was used as only organosilicon precursor. It is remarkable that the experimental C/N molar ratios obtained for these solids were close to theoretical C/N molar ratio, which depends on their composition in the synthesis gel. This fact would indicate that the organosilicon precursors (APTMS) were preserved during the hydrothermal synthesis process. In the case of x-MLHM-SH materials, the chemical analysis also showed an increasing in sulfur content when the amount of MPTMS precursor was growing in the synthesis gel (Table S2). However, in these materials, when the percentage of MPTMS was inferior to 30% respect total SiO_2 moles, the experimental C/S molar ratios obtained for these materials were far to theoretical C/S molar ratio, due to a lower incorporation of MPTMS in the framework of the hybrid materials. Finally, hybrid solids obtained from the combination of APTMS, MPTMS and TEMS as organosilicon precursors, x-MLHM-NH_2-SH (Table S3), showed similar experimental and theoretical C/N and C/S molar ratios, especially for aminosilyl precursor, such as it was above described for x-MLHM-NH_2

materials. Therefore, from the data obtained through the organic content, it was possible to confirm that, in general, organosilane precursors, used during the synthesis process, were finally incorporated into the framework of the hybrid materials. Thus, these results showed the high effectiveness of the one-pot hydrothermal synthesis to incorporate organic structural fragments during the synthesis of the monolayered hybrid materials.

When oxidation treatments were performed in order to convert thiol groups in acid sites for x-MLHM-SH and x-MLHM-NH_2-SH materials, the chemical composition remained practically invariable, confirming that the nature of the organic-inorganic materials after the acid post-synthesis processes was maintained (Tables S4 and S5). This was also confirmed from X-ray diffractograms of the acid materials, such as it was previously commented (Figures S3 and S4).

Figure S7 shows thermogravimetrical analyses (TGA) and the corresponding derivate curves curves (DTA) for the as-synthesized monolayered organic-inorganic materials obtained using 100% TEMS, 30% APTMS, 30% MPTMS and 30%MPTMS together with 30%APTMS, respectively, respect to total SiO_2 mol. The results allowed establishing the hydrothermal stability of organic units introduced in the layered solids. In all cases, besides the first weight loss due to the hydration water, it is observed a main weight loss assigned to organic moieties from the organosilane precursors (APTMS, MPTMS and TEMS) used in the synthesis route. In addition, from DTA curves, it was estimated the thermal stability of the organic units included in the framework of hybrid solids. It is observed that methyl groups exhibit the highest stability, breaking down at temperatures in the 450 – 550 ºC range (100-MLHM-TEMS, Figure S7a), whereas amino/thiolpropyl fragments showed a lower hydrothermal stability (250 – 450 ºC), such as it is showed in Figures S7 b, c and d. Definitively, these results showed the high effectiveness of the one-pot hydrothermal procedure to incorporate organic fragments, utilized during the synthesis of the lamellar hybrid materials from organosilane precursors, being stable up to 250ºC when amino and/or thiol groups were incorporated.

Spectroscopic characterization: NMR spectroscopy

^{13}C CP/MAS NMR chemical shifts of the organic-inorganic hybrid solids are included in Figure 4. The spectra corroborated the effective presence of organic fragments in the lamellar framework of the hybrid materials. The results indicated the total preservation of the organic moieties situated in the interlayer space after the hydrothermal synthesis route, since all carbon atoms, also the carbon atoms directly linked to silicon, are undoubtedly assigned in the spectra. This observation confirmed that methyl and amino/thiol-sulfonic propyl pending units remain intact as in the initial organosilane precursors, evidencing the presence of Si-bonded carbon species in the lamellar solids. It is remarkable that, in all samples, the bands assigned to alkoxide groups present

in the initial monosilane precursors were not detected (except for 30-MLHM-NH_2, Figure 4b), confirming that hydrolysis of all alkoxy terminal groups of the organosilicon monomers was completed during the hydrothermal direct synthesis. The effective oxidation treatment was also confirmed by NMR (Figure 4d and 4f), being observed at ~ 58 ppm the chemical shift associated to sulfonic groups covalently bonded to propylsilane units from MPTMS precursor. However, for 30-MLHM-SO_3H material (Figure 4d), chemical shifts associated to thiol and sulfonic groups were observed, not being all thiol groups oxidized to sulfonic acids during oxidation process. On the other hand, an additional band assigned to nitro groups was observed at ~ 65 ppm (Figure 4f), which would be consequence of the oxidation of amino groups from APTMS, due to strong acid conditions used during the oxidation treatment (Figure S8). The rest of the chemical shifts associated to carbon atoms of the pending groups remaining without changing.

From the ^{13}C CP/MAS NMR chemical shifts, we were able to confirm that organic units preserved their integrity after the one-pot hydrothermal process. Then, by means of ^{29}Si MAS NMR, we corroborated that the organic fragments not only remained unbroken but were also introduced covalently into the layered network, being connected to tetrahedral silica units and placed between consecutive layers in the interlayer region. Figure 5 shows the ^{29}Si BD/MAS NMR spectra of different organic–inorganic layered materials prepared starting from several organosilane precursors. In all cases, characteristic bands located from -60 ppm to -80 ppm, due to T-type silicon species containing Si–C bond, were identified. However, the broadness of the main band due to T silicon atoms (C-$Si(OH)_x(OAl)_{3-x}$, x=0-2), does not allow to distinguish separately individual T^1, T^2 and T^3 silicon species, except for 100-LHM-TEMS sample, which present one sharp band assigned to T^1 silicon species and other clearly broader associated to T^2 and T^3 units. These results would be indicative that, in this latter case, the poly-condensation of organosilicon monomers could not be complete, being detectable the existence of several silanol groups on the external surface of the silicoaluminate sheets, associated with the defects generation in the structure.

It is remarkable the absence of Q-type silicon atoms in the synthetized hybrid materials, assigned to tetrahedral silicon species included in highly siliceous materials. This confirms that cleavage of Si-C bond does not exist during the direct alkaline hydrothermal synthesis route and neither after acid oxidation carried out in order to convert thiol groups in sulfonic acid units.

Additional confirmation of the integration of organic moieties into the lamellar hybrid solids by bonding to inorganic units, come from ^{29}Si NMR spectra of pure organosilane starting monomers (APTMS, MPTMS and TEMS). Frequently, the pure organic-inorganic monomers present only one chemical shift due to silicon atoms focused between -40 ppm and -60 ppm (T-type), in function of the pending organic group (propylamino at ~-45.7 ppm, propylthiol at ~-42.5 ppm and methyl groups at ~-43.5 ppm). When these organic fragments are finally connected to the framework in

the hybrid layered material, the chemical shift assigned to silicon atoms linked to carbon units goes from -60 ppm – -80 ppm. This fact confirms the effective introduction of organic fragments into the final lamellar hybrid solids (see scheme in Figure 5).

Textural properties

Nitrogen adsorption isotherms of the monolayered hybrid materials (MLHM) showed standard type II isotherms, assigned to solids with reduced porosity (Figure S9). For this, the hybrid solids exhibited a BET specific surface area close to 100 m^2g^{-1} and a pore volume around to 0.30 cm^3g^{-1}. In these lamellar materials, the high concentration of organic fragments situated in the interlayer region does not favor the generation of porous cavities with elevated dimensions between the inorganic layers, which could to be the reason of the reduced specific surface area of the lamellar hybrid solids here prepared. Furthermore, the marked hydrophobic character of the MLHM materials difficult the optimal gas adsorption between the monolayers. On the other hand, intracrystalline porosity, delimited by pores of six member rings (6MRs), structuring each single silicoalumina sheet[34, 44], is not detectable from gases adsorption measurements. So, these factors hinder the correct estimation of textural properties related with the hybrid lamellar solids, being difficult to calculate the exact pore size distributions.

Valorization of base and acid sites

The presence of base sites located in the interlayer space due to pending amino groups from APTMS, which was used as organosilicon precursor for 30-MLHM-NH_2 and 30-MLHM-NH_2-SO_3H samples, was determined by means of the desorbed CO_2 by thermoprogrammed desorption technique (TPD) (Figure S10). Specifically, both samples showed a common CO_2 desorption band, approximately at 400-650ºC, desorbing 30-MLHM-NH_2 base catalyst around 128 cm^3 CO_2 g^{-1} whilst 30-MLHM-NH_2-SO_3H bifunctional hybrid catalyst desorbed 60 cm^3 CO_2 g^{-1}, since some nitro species were formed after acid oxidation treatment, such as was confirmed from NMR spectra (Figure 4f).

Additionally, by means of the desorbed ammonia by TPD technique, it was possible to estimate the presence of acid sites located in the interlayer space due to pending sulfonic groups, because of thiol groups oxidation from MPTMS used as organosilicon precursor during the hydrothermal synthesis (Figure 6). Specifically, all samples have a common ammonia desorption band, approximately at 300-500ºC (marked as range 2 in Figure 6), associated to ammonia molecules that interact with the tetrahedral aluminum present in the organic-inorganic sheets, forming part of the framework. Furthermore, the oxidized samples, 30-MLHM-SO_3H and 30-MLHM-NH_2-SO_3H, showed a specific desorption ammonia band at higher temperature, around 500-700ºC, assigned to sulfonic groups, emphasizing the high strength of this type of acid sites (range 3 in

Figure 6). On the other hand, another band with lower intensity is also observed, at approximately 200ºC, probably due to slight contribution of weak acid sites assigned to ammonia molecules interacting with surface silanol groups, mainly as a consequence of the formation of the defects after the oxidation treatment (range 1 in Figure 6). Definitively, the characterization data obtained from TPD analyses, which are summarized in Table S6, clearly corroborate the possibility to obtain well-defined monolayered hybrid materials with accessible pending base and acid sites located between two contiguous individual nanosheets.

Catalytic activity

Base catalysis

With the objective to investigate the accessibility to the reactants and the reactivity of x-MLHM-NH_2 hybrid materials as base catalysts, containing pending interlayered propylamino moieties, their catalytic performance was tested through the condensation of carbonyl compounds with active methylenic substrates, in reactions such as Knoevenagel and Henry, which implies an key tool in organic chemistry for C-C bond formation and for the synthesis of substituted alkenes products. These latter are of interest as end-products and intermediates for the production of fine chemicals and commodities, such as perfumes, pharmaceuticals and polymers,[47-51] thanks to their properties as enzyme inhibitors, antitumor, anti-inflammatory and antibacterial agents.[52-55]

Knoevenagel Condensation

This condensation reaction can be catalyzed by strong and weak base active sites depending on the level of activation of the substrate containing methylenic activated groups. The kinetic of the Knoevenagel reaction is generally considered to be first order with respect to each reactant and the catalyst.[48-51, 56] In this work, the reactions between benzaldehyde and different activated methylene groups with increasing pK_a values, 11 and 13, corresponding to ethylacetoacetate and diethyl malonate, respectively (Scheme 1), were carried out to estimate the level of basicity achieved within these MLHM materials. In Figure 7, it can be observed that the ethyl 2-benzylidene acetoacetate was successfully performed in presence of 30-MLHM-NH_2 and 50-MLHM-NH_2, which produced a similar yield of 86% after 7 h of reaction time. However, when the reaction was performed with 100-MLHM-NH_2, that contained the highest amino groups loading, the yield was only 61% after 7 h of reaction time. The low crystallinity and homogeneity level achieved in the framework due to the excess of organic moieties located in the interlayer region (Figure S1f) and consequently, hindering the access to the reactants, together with an decreasing in the strength of the base sites due to the high number of active sites,[57, 58] can be responsible for the lower activity of 100-MLHM-NH_2 in this test reaction. On the other hand, 100-MLHM-TEMS, which

does not contain amino pending groups, only methyl groups, hardly produced a 0.6% of yield in the same reaction time. Furthermore, it was confirmed that cationic sodium species, which act as compensators of the negative charge due to aluminum tetrahedral coordinated into the framework of organic layers, did not exhibit base catalytic activity. The turnover frequencies calculated after 1 h, initial rates and kinetic constants are reported in Table S7, being observable that the catalytic performance of x-MLHM-NH_2-type materials is comparable with a known active base mesoporous hybrid materials containing strong guanidine proton sponges,[59] which acted as functional building blocks. Therefore, it can be concluded that 50% APTMS was the optimum percentage of moles silanes employed during the synthesis respect total SiO_2 moles, to obtain the most active catalyst to carry out this base condensation reaction.

Since the best performance in the prior Knoevenagel condensation was carried out by 30-MLHM-NH_2 and 50-MLHM-NH_2 materials, these base hybrid materials were studied in the diethyl malonate condensation, which involves more demanding methylenic reagents. In this case, diethyl 2-benzylidenemalonate was successful obtained for both hybrid materials with a yield of ~ 80% after 30 h of reaction time (Figure S11).

Henry reaction

x-MLHM-NH_2 hybrid materials were evaluated in Henry reaction, a condensation reaction of nitroalkanes with carbonyl compounds to produce nitroalkenes (Scheme 2), which are interesting for the synthesis of pharmaceutical products.[60, 61] However, the selective formation of nitroalkene (**2**)**,** using conventional strong bases, is difficult to achieve since the conjugate addition of the nitroalkane to the C-C double bond of the nitroalkene facilitates the formation of bis-nitro compounds, favoring low yields associated to dimerization or polymerization processes (product **3**, Scheme 2).[62-64]

The Henry reaction between benzaldehyde and nitromethane (p*Ka* = 10.2) was performed with the hybrid materials which reached the highest yields for Knoevenagel condensations, 30-MLHM-NH_2 and 50-MLHM-NH_2. Moreover, 100-MLHM-TEMS, which did not contain pending amino groups, was also used to study the catalytic influence due to the absence of base units into the framework. From the yields of nitrostyrene (**2**) reported in Figure 8, it is observed that the 50-MLHM-NH_2 material exhibited the best catalytic performance, reaching 98% of yield and 99% selectivity towards desired product **2** (nitrostyrene) after 3 h. In this reaction, 30-MLHM-NH_2 showed lower initial catalytic activity, achieving yields of 97% after 5h of reaction time. Such as it was expected, 100-MLHM-TEMS did not show any activity in the nitrostyrene´s production. Similarly to previous Knoevenagel condensations, turnover frequencies calculated after 2 h, initial rates and kinetic constants are reported in Table S8, being confirmed that 50-MLHM-NH_2 catalyst

exhibited catalytic activity similar to known base mesoporous hybrid materials containing in the framework guanidine proton sponge moieties taken as reference solid organic-inorganic catalysts.[59]

Eventually, from these results, it is confirmed that pending propylamino groups included in the lamellar hybrid solids are accessible to reactants and active to catalyze processes where relatively strong base sites are necessary. In particular, 50-MLHM-NH_2 material showed the best performance as heterogeneous base catalyst in this type of reactions for C-C bond formation.

Acid catalysis

Acetalization of benzaldehyde with methanol

Formation of acetals is one of the most important protecting methods for carbonyl compounds[65], and a large of amount of synthetic work has been done on the protection of the carbonyl group. Acetals are important in carbohydrate[66] and steroid chemistry.[67, 68] Furthermore, in the pharmaceutical,[69] phytopharmaceutical, fragance[70] and lacquer industries, acetals are used both as intermediates and as final products. The most general method for the synthesis of acetals is by means of the reaction of carbonyl compounds with an alcohol or an ortho ester in the presence of acid catalysts.

In this study, the results obtained on acetalization of benzaldehyde with methanol to 1,1-dimethoxytoluene (Scheme 3), catalyzed by x-MLHM-SO_3H as acid heterogeneous catalyst, are presented in Figure 9. It was found that 100-MLHM-SO_3H showed the best catalytic activity, which resulted in a yield of 80% after 24h of reaction. It was also observed that, 50-MLHM-SO_3H and 30-MLHM-SO_3H, with less than half of thiol groups respect to 100-MLHM-SO_3H, produced conversions slightly lower to desired product, reaching values around 77% and 66% after 24 h of reaction, respectively. On the other hand, in absence of sulfonic groups, i.e, when 100-MLHM-TEMS hybrid material and blank experiment were studied, the desired product was obtained with inferior yields to 3%. These results show that the x-MLHM-SO_3H hybrid catalysts can act as effective acid catalysts for aldehydes acetalization, although not all thiol groups were oxidized to sulfonic groups, such as it is observed by ^{13}C CP/MAS NMR spectrum of 30-MLHM-SO_3H catalyst (Figure 4d), where a mixture between pending sulfonic and thiol groups, due to an incomplete oxidation, are detected.

One-pot tandem cascade reaction

Deacetalization-Knoevenagel condensation

The use of only one solid catalyst that contains different active functions to catalyse the individual reaction steps of tandem, consecutive or cascade reactions, avoiding the isolation of intermediate products, their purification and solvent removal, should favour the development of more sustainable chemical processes, saving energy and increasing the global efficiency.[71]

In this case, the bifunctional acid-base hybrid catalysts (x-MLHM-NH_2-SO_3H), here studied, were studied in a one-pot two-step reaction that involved an acetal hydrolysis followed by Knoevenagel condensation (Scheme 4). Catalytic experiments were carried out to investigate how the acid and base functionalities of the hybrid materials cooperate positively between them. The first step is the deacetalization of the benzaldehyde dimethylacetal (1) to benzaldehyde (2), which, in second step, reacts with ethyl cyanoacetate (3) to give the final product, ethylcyanocinnamate (4). In Figure 10 (a, b and c) the catalytic activity of the different bifunctional hybrid catalysts is reported, where the evolution for each reagent during the tandem reaction is shown. From the results, it is observed that 30-MLHM-NH_2-SO_3H hybrid material performed successfully the one-pot two-step reaction, obtaining a yield of 92% of the final product with 98% selectivity, after 18 h of reaction time. However, 50-MLHM-NH_2-SO_3H and 15-MLHM-NH_2-SO_3H hardly reached yields to the final product close to 25% in the same reaction time, where the second step (Knoevenagel condensation) was evidenced as limit step, since for these two solid catalysts, a slow transformation from intermediate benzaldehyde to final product (4) was observed (Figure 10b). Therefore, it is concluded that the optimal percentage of silane moles in the synthesis gel for each monosilane precursor is 30% APTMS, 30% MPTMS and 40% TEMS, to obtain the most active MLHM catalyst for this type of tandem reaction, which is probably due to insufficient amount of active acid and base sites of 15-MLHM-NH_2-SO_3H and an excess of organic moieties in the interlayer space that hampers the accessibility to the reactants, in the case of 50-MLHM-NH_2-SO_3H.

In order to confirm the synergistic cooperation from acid and basic functionalities, the same one–pot reaction was performed with others hybrid materials which only contained an unique functionality in the framework (Table 1), such as 30-MLHM-NH_2 (amino groups), 30-MLHM-NH_3^+ (ammonium groups), 30-MLHM-SO_3H (sulfonic groups) and 100-MLHM-TEMS (without active sites). When only amino groups were involved in the tandem reaction (Table 1, entry 2), using 30-MLHM-NH_2 hybrid material, deacetalization did not occur, since acid sites are necessary to produce benzaldehyde. Thus, conversion of the starting reagent barely was 2.7%, and the final product only was produced with 1.2% yield. Low conversions were also obtained when protonated amino groups were used as catalyst for the tandem reaction (30-MLHM-NH_3^+), which allowed to study the catalytic reactivity of pending protonated amine groups. In this case (Table 1, entry 3), slightly higher conversion of benzaldehyde dimethylacetal was obtained respect to non-protonated amino groups, since some acid species could be released at the reaction medium. Nevertheless, benzaldehyde just was produced with a 12.9% yield and only a 1.4% yield was obtained for the final product (4). On the other hand, when solely sulfonic groups are involved in one-pot cascade reaction, 30-MLHM-SO_3H (Table 1, entry 4), benzaldehyde was successfully obtained with a yield of 90.1%, whilst only 3.4% of final product was achieved, due to the absence of base sites, which are

indispensable for final Knoevenagel condensation. When 100-MLHM-TEMS was used as catalyst (Table 1, entry 5), benzaldehyde was obtained with 52.1% yield, probably due the acidity related to the existence of several silanol groups on the external region of the organic-inorganic sheets. However, this hybrid material, without amino and sulfonic moieties, was not able to perform the Knoevenagel condensation and the final product was produced with only 8.5% yield. Finally, a blank experiment was performed (Table 1, entry 6) and the results showed that, under these conditions, the Knoevenagel condensation did not occur successfully either (yield of 33.8% after 18h). Definitively, these results corroborate that each catalyst (acid and base) on its own is unable to perform the one-pot tandem reaction, confirming that a positive cooperative behavior of the acid-base hybrid catalysts when different active centers are located in the same network, such as exists in enzymatic processes.[72] Similarly to previous discussed catalytic tests, initial rates and kinetic constants reported in Table 1 showed that catalytic performance of 30-MLHM-NH_2-SO_3H material is comparable with that exhibited by known bifunctional acid-base mesoporous hybrid catalysts (Table 1, entry 7),[73] containing both base proton sponges (derived of 1,8-bis(dimethylamino)naphthalene (DMAN) compounds) and acid sulfonic groups into the framework. This comparison confirms the validity of bifunctional lamellar hybrid catalysts (x-MLHM-NH_2-SO_3H) to be used as active acid-base catalysts for one-pot two-step tandem processes.

Catalyst recyclability

Catalyst deactivation and reusability was studied with the acid-base bifunctional 30-MLHM-NH_2-SO_3H catalyst in the one-pot cascade reaction of deacetalization-Knoevenagel condensation, which was already above described (Figure 10), during 5 successive uses (Figure S12). After each experiment, the catalyst was filtered with ethanol, dried at 60ºC and reused. The results confirmed that the hybrid catalyst is recycled, being only observable a slight loss in activity after five consecutive catalytic uses.

XRD pattern (Figure S13), ^{13}C CP/MAS NMR spectrum (Figure S14) and elemental analysis of the used 30-MLHM-NH_2-SO_3H catalyst confirmed the stability and integrity of the lamellar organic-inorganic framework after five catalytic cycles. Specially, in Figure S13, it is observed that the first *(100)* diffraction band characteristic of ordered lamellar materials was still present after five consecutive catalytic performances, verifying that the lamellar morphology was preserved. Moreover, chemical shifts obtained by ^{13}C CP/MAS NMR spectroscopy for the organic-inorganic hybrid material, after being employed as reusable acid-base catalyst, are shown in Figure S14. Both samples (fresh and reused catalyst) displayed similar spectra, confirming the preservation of the organic fragments present in the material after several catalytic cycles. However, reused 30-MLHM-NH_2-SO_3H material showed additional bands associated to the adsorbed final product (4) of the

one-pot tandem reaction (see inset in Figure S14), confirming that some molecules of this product was adsorbed over the hybrid material.

Moreover, to verify the heterogeneous catalytic character of 30-MLHM-NH_2-SO_3H solid, a leaching test was performed in the tandem cascade reaction. So, when reaction time was 3 h, solid catalyst was filtered from the reaction mixture and the reaction in absence of solid catalyst was continued. After 15 h, the product formation was hardly increased, just from 32.5% to 36.5% of yield (Figure S15). Hence, it can be concluded that the catalysis occurs in solid phase and leaching effect of active species from solid catalyst to liquid reaction medium is not observed.

Thus, the catalytic results showed the validity of these monolayered hybrid solids to be used as effective and reusable acid-base catalysts, considering the reactivity of the heterogeneized and stabilized active sites situated between silicoaluminate sheets. Specifically, the use of 50% SiO_2 mol of APTMS, 50% SiO_2 mol of MPTMS or 50-60% SiO_2 mol if both precursors are combined during the hydrothermal synthesis, favored the formation of most active MLHM-type catalysts for C-C bond forming reactions and associated tandem reactions where acid, base or cooperative acid-base active sites are necessary.

Conclusions

Novel bifunctional acid-base monolayered hybrid catalyst (MLHMs), based on ordered organic aluminosilicate sheets with amino and sulfonic pending active groups, have been successfully prepared by direct alkaline hydrothermal synthesis and tested in consecutive catalytic transformations.

The direct intercalation of pending amino and thiol organic groups, from suitable organosilicon precursors (APTMS and MPTMS) located in the interlayer space of individual layers, together with the effective oxidation treatment of thiol groups without protecting base groups and without modifying the layered characteristics of the solids, were important to generate organic-inorganic materials with acid-base character.

The successful cohabitation of acid and base groups and their good performance as acid-base catalysts was evaluated in one-pot two-step processes that involved an acid-catalyzed acetal hydrolysis followed by a base-catalyzed Knoevenagel reaction. The obtained results imply a significant advance in the preparation of novel bi-functional hybrid organic-inorganic solids based on single organic silicoaluminate sheets with different stabilized functions in the interlayer space, opening the possibility to generate further multifunctional solids from suitable organosilicon precursors through direct hydrothermal synthesis.

Acknowledgments

The authors thank financial support to Spanish Government by MAT2014-52085-C2-1-P and Severo Ochoa Excellence Program SEV-2012-0267. AG thanks pre-doctoral fellowships from MINECO for economical support (reference number BES-2012-052429)**.** The European Union is also acknowledged by ERC-AdG-2014-671093-SynCatMatch.

Supporting Information.

Chemical analysis, X-ray diffractograms (XRD), thermogravimetical curves (TGA) and their corresponding derivatives (DTA), nitrogen adsorption isotherms, CO_2-TPD, NH_3-TPD and TEM micrographs of the MLHM hybrid materials. TOFs, initial rates and kinetic constants for the Knoevenagel condensation and the Henry reaction between benzaldehyde and ethyl acetoacetate or nitromethane, respectively, when are performed by x-MLHM-NH_2 catalysts. Diethyl malonate condensation performed by x-MLHM-NH_2 catalysts. Catalytic recycles and leaching test for 30-MLHM-NH_2-SO_3H material when is used as bifunctional catalyst in the one-pot two-step reaction (deacetalization-Knoevenagel condensation). X-ray diffractograms (XRD) and ^{13}C CP/MAS NMR spectra of the reused 30-MLHM-NH_2-SO_3H catalyst, after using as bifunctional catalyst in the tandem process.

Tables

Table 1. One-pot acetal hydrolysis-Knoevenagel condensation tandem reaction using ethyl cyanoacetate during 18 h of reaction time with 5 mol % of N.

Entry	Catalyst	Convers. of (1)(%)	Yield of (2)(%)	Yield of (4)(%)	r_0(mol·L^{-1}·h^{-1})	k(h^{-1})
1	30-MLHM-NH_2-SO_3H	97.0	4.5	91.9	58.2	0.58
2	30-MLHM-NH_2	2.7	1.5	1.2	0.38	$3.84\cdot10^{-3}$
3	30-MLHM-NH_3^+	15.1	12.9	1.4	0.55	$5.53\cdot10^{-3}$
4	30-MLHM-SO_3H[a]	93.5	90.1	3.4	43.3	0.433
5	100-MLHM-TEMS[b]	60.6	52.1	8.5	3.83	0.0383
6	blank	82.1	45.2	33.8	17.7	0.18
7	DMAN-Sulfonic[c] Hybrid Material	100	2	98	24.3	0.24

[a] Tandem reaction with 4 mol% of S, mol% fixed by the 30-MLHM-NH_2-SO_3H bifunctional catalyst . [b] Tandem reaction performed using the same weight of catalyst (mg) added for 30-MLHM-NH_2-SO_3H catalyst. Benzaldehyde dimethylacetal (2.17 mmol), ethyl cyanoacetate (2.01 mmol) and H_20 (18 µL) at 90ºC. [c] Corresponding to DMAN-SO_3H-SiO_2-5-5 sample from reference (73), being DMAN 1,8-bis(dimethylamino)naphthalene. Reaction conditions: Benzaldehyde dimethylacetal (5.45 mmol), ethyl cyanoacetate (5.24 mmol) and H_20 (30 µL) at 80ºC with 0.25 mmol of base sites.

Schemes

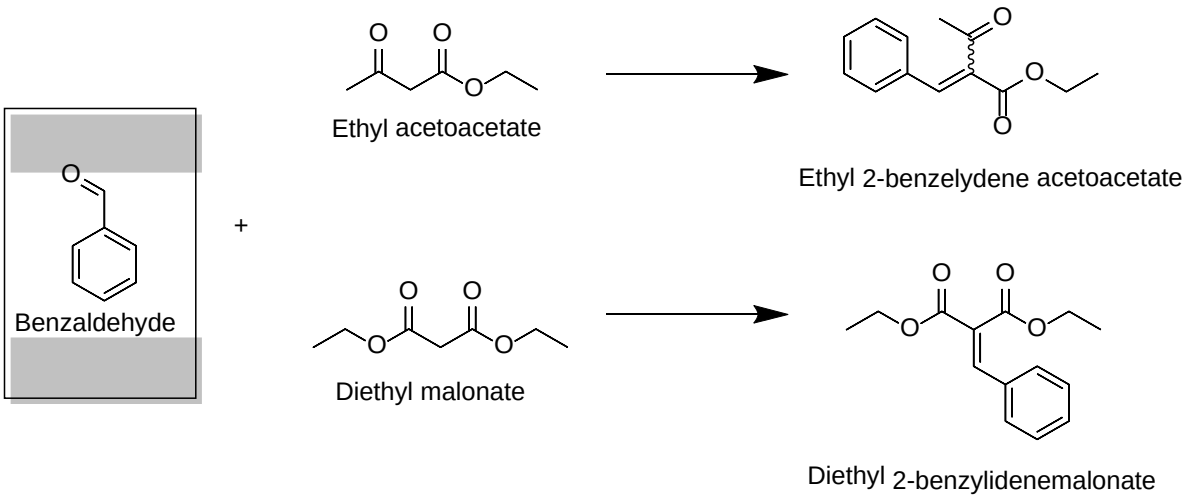

Scheme 1. Knoevenagel condensation between benzaldehyde and different base-strength demanding substrates.

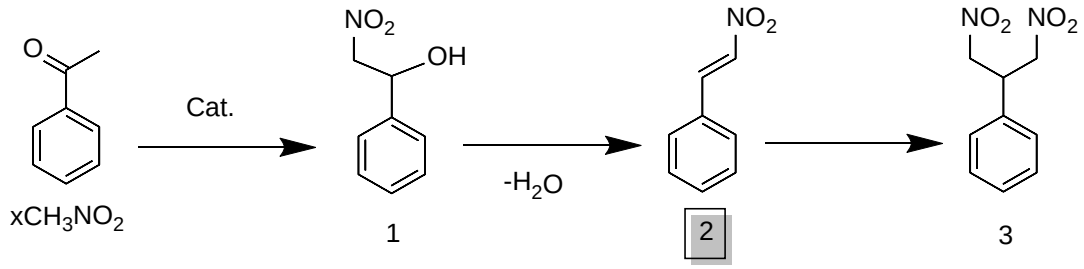

Scheme 2. Henry reaction between benzaldehyde and nitromethane.

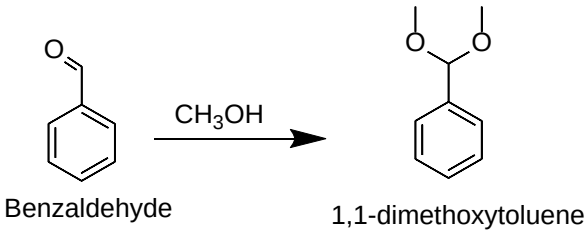

Scheme 3. Acetalization of benzaldehyde with methanol to 1,1-dimethoxytoluene**.**

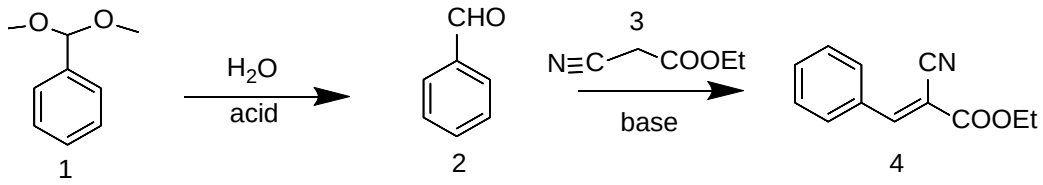

Scheme 4. One pot hydrolysis-Knoevenagel condensation cascade reaction.

Figures

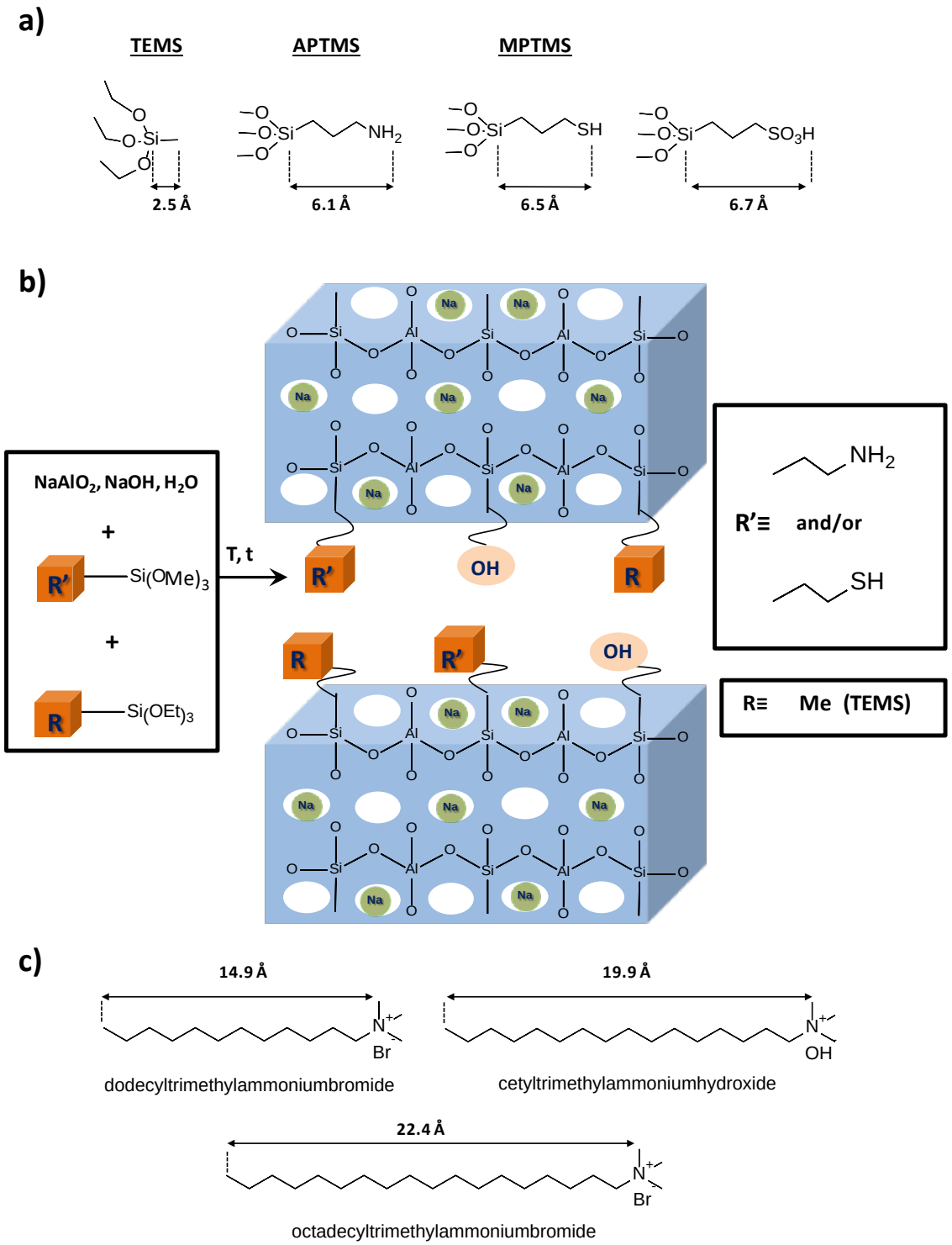

Figure 1. (a) Monosilanes used as organosilica precursors: TEMS (triethoxymethylsilane), APTMS (3-aminopropyl)trimethoxysilane, MPTMS (3-mercaptopropyl)trimethoxysilane and oxidized MPTMS. (b) Synthesis route followed to obtain the monolayered hybrid materials (MLHM). (c) Surfactants agents used to prepare the swollen MLHM materials.

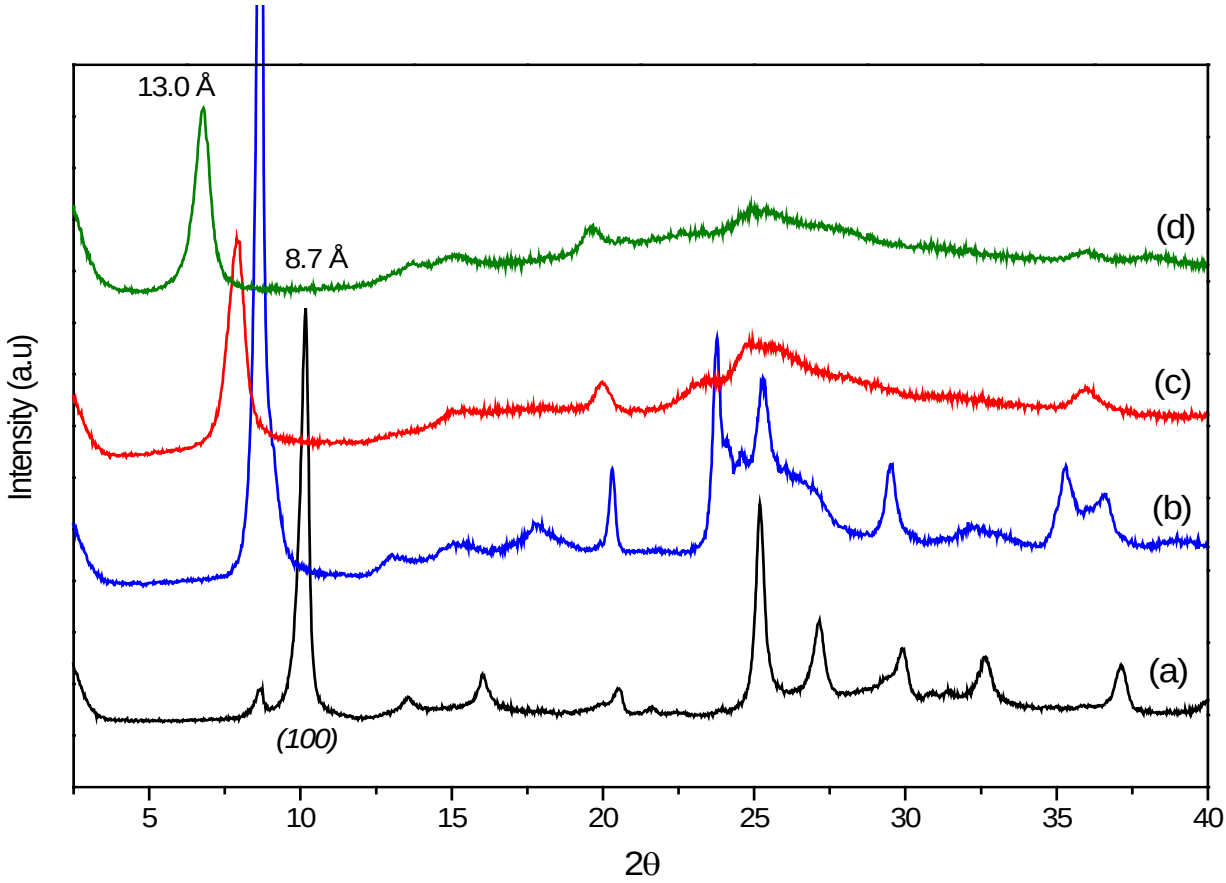

Figure 2. X-ray diffractograms (XRD) of hybrid monolayered materials x-MLHM-NH_2-SH: (a) 100-MLHM-TEMS, (b) 15-MLHM-NH_2-SH, (c) 30-MLHM-NH_2-SH and (d) 50-MLHM-NH_2-SH.

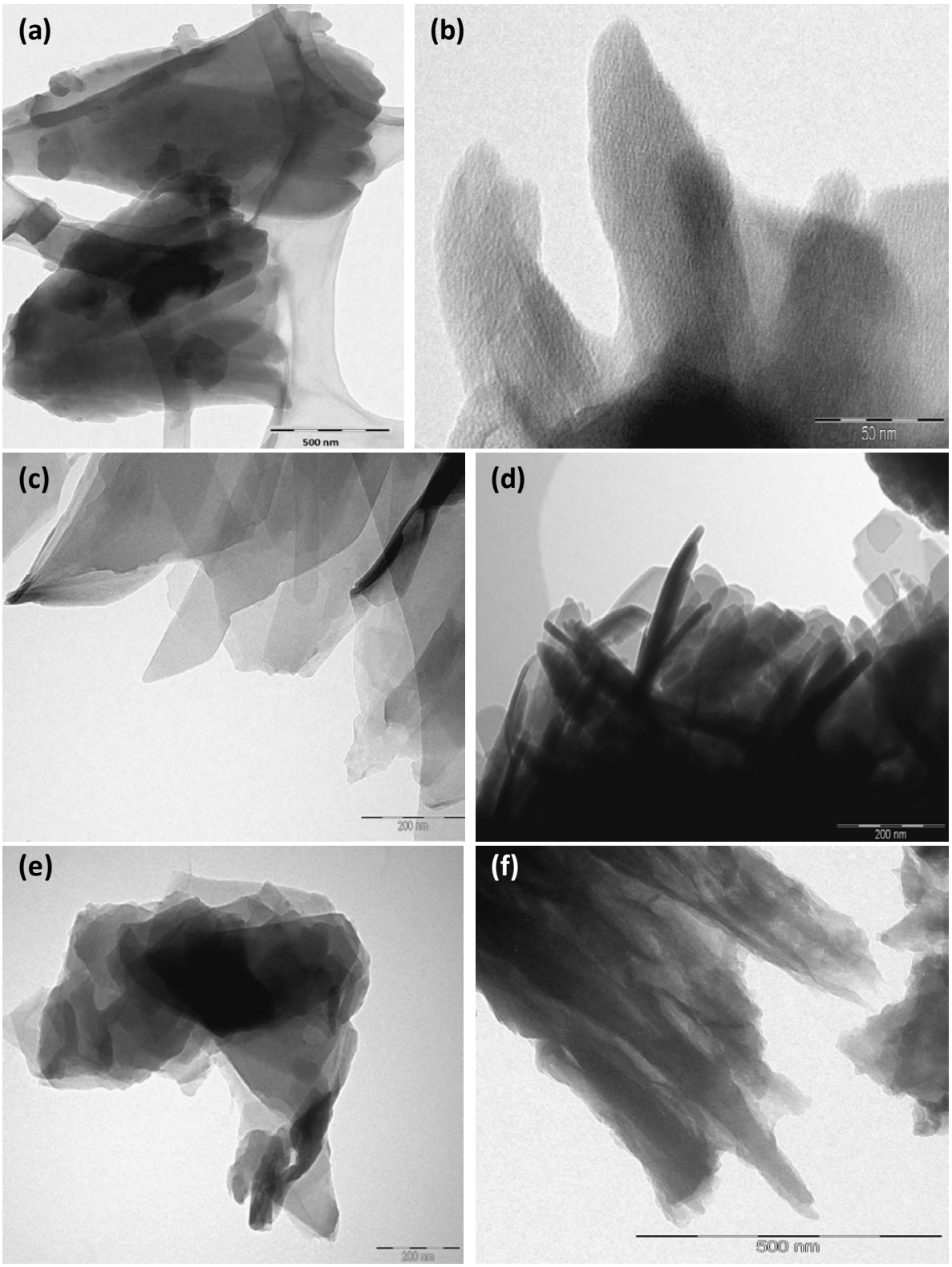

Figure 3. TEM micrographs of monolayered organic-inorganic materials: (a) and (b) 100-MLHM-TEMS, (c) 30-MLHM-SH, (d) 30-MLHM-SO_3H, (e) 30-MLHM-NH_2-SH and (f) 30-MLHM-NH_2-SO_3H. The reference bars correspond to 500 nm for (a) and (f), 50 nm for (b) and 200nm for (c), (d) and (e) micrographs.

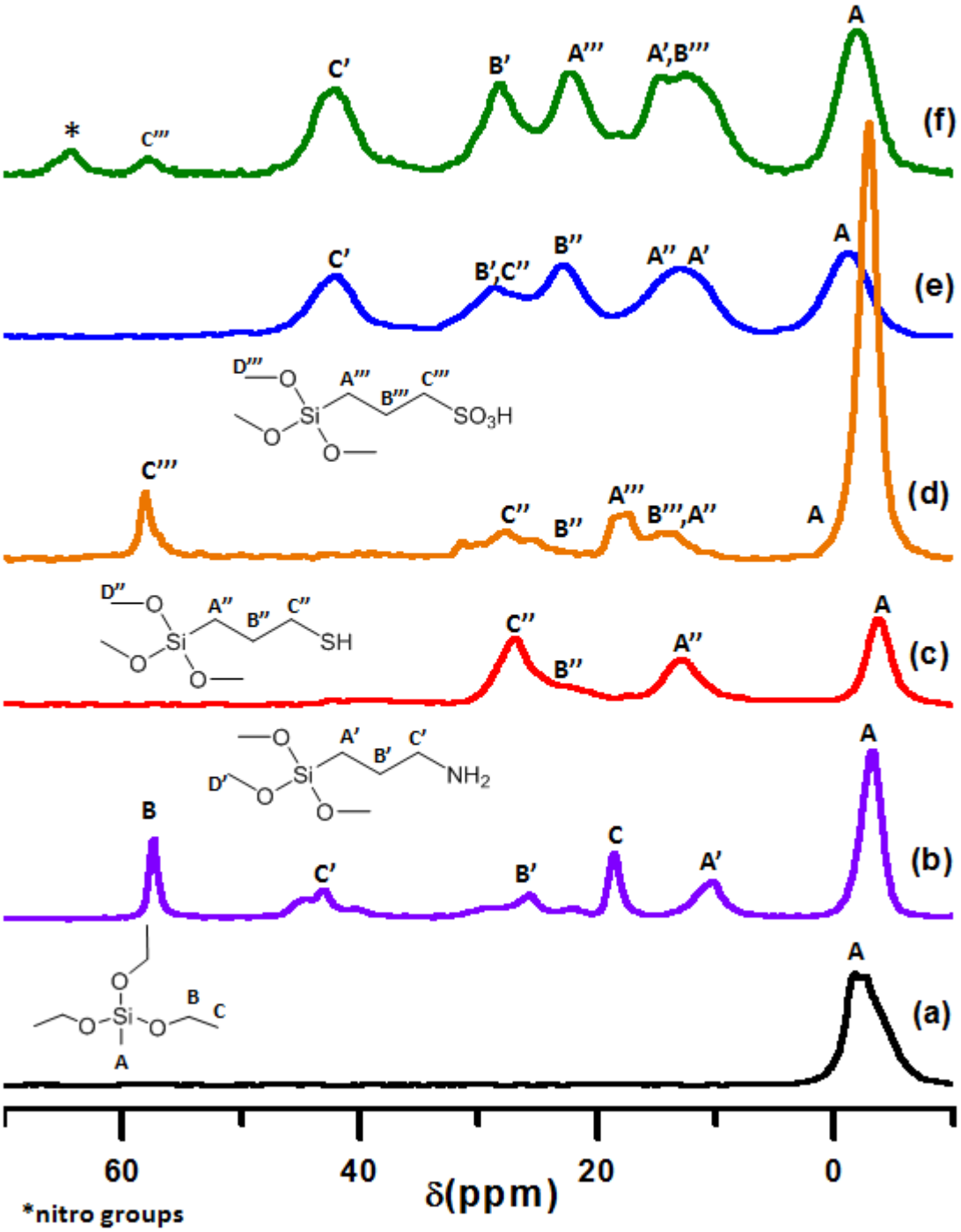

Figure 4. ^{13}C CP/MAS NMR spectra of different monolayered hybrid materials, showing the assignment of the chemical shifts with the carbon atoms contained into the solids: (a) 100-MLHM-TEMS, (b) 30-MLHM-NH_2, (c) 30-MLHM-SH, (d) 30-MLHM-SO_3H, (e) 30-MLHM-NH_2-SH, (f) 30-MLHM-NH_2-SO_3H.

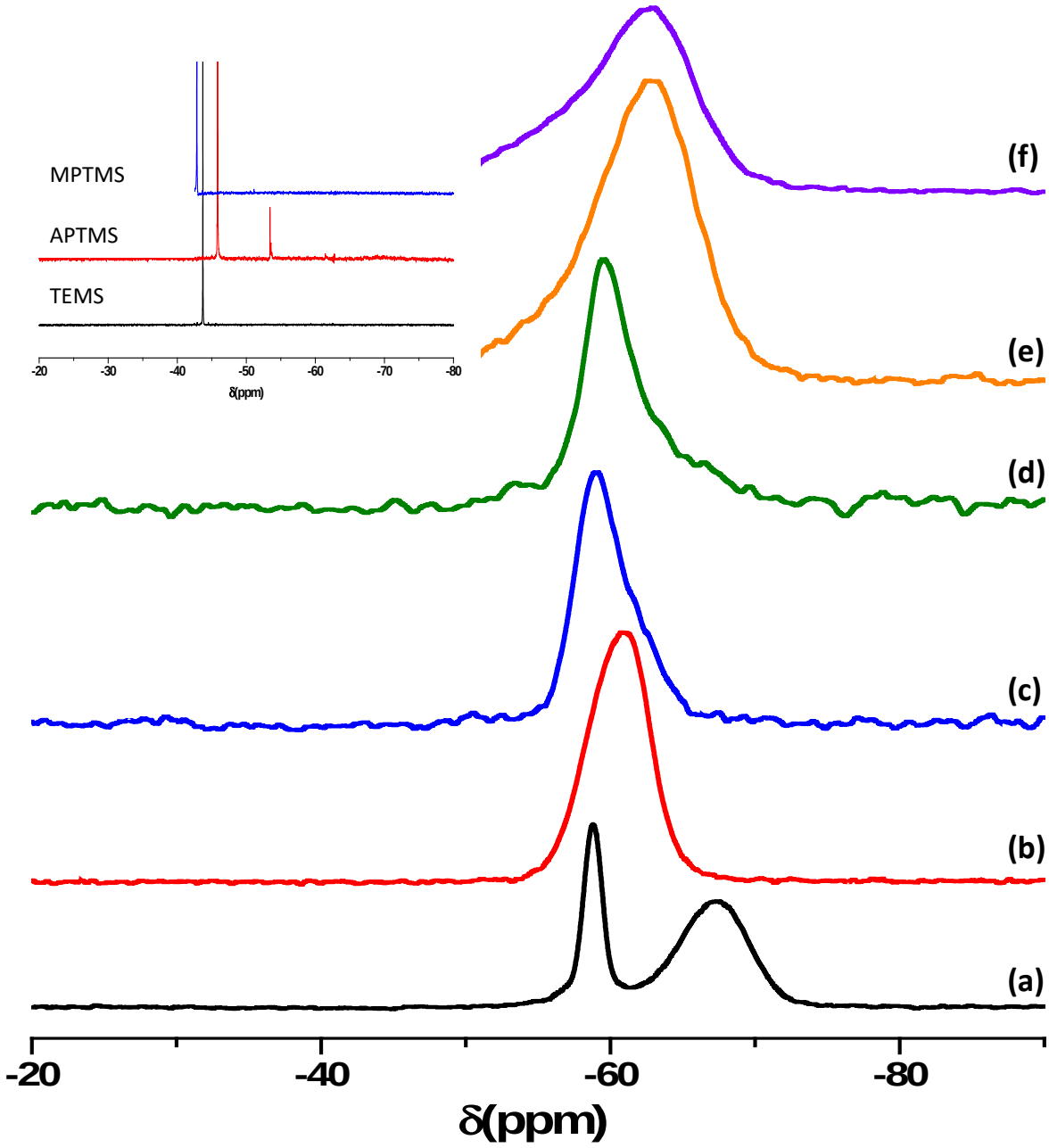

Figure 5. ^{29}Si BD/MAS NMR spectra of different monolayered hybrid materials: (a) 100-MLHM-TEMS, (b) 30-MLHM-NH_2, (c) 30-MLHM-SH, (d) 30-MLHM-SO_3H, (e) 30-MLHM-NH_2-SH, (f) 30-MLHM-NH_2-SO_3H.In the inset, ^{29}Si BD/MAS NMR spectra of pure monosilane precursors are shown.

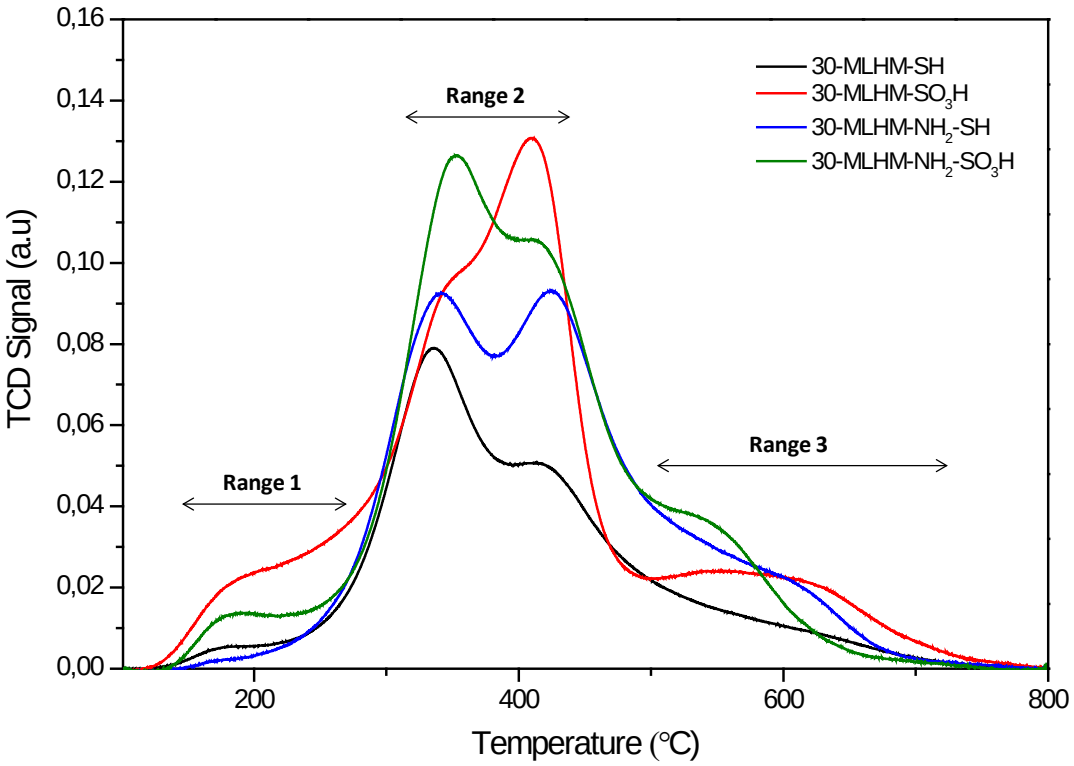

Figure 6. NH_3 thermoprogrammed desorption curves of layered hybrid materials: (black) 30-MLHM-SH, (red) 30-MLHM-SO_3H, (blue) 30-MLHM-NH_2-SH and (green) 30-MLHM-NH_2-SO_3H.

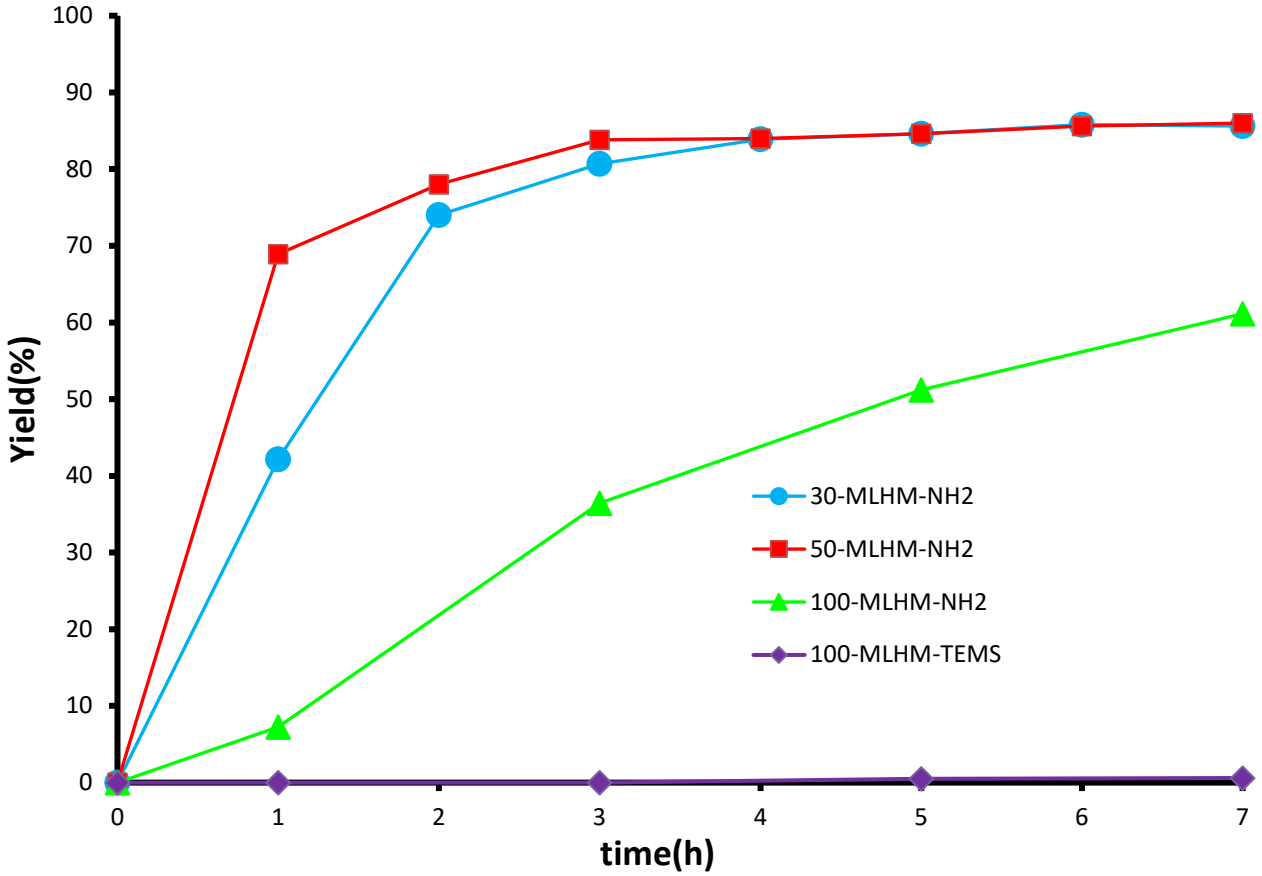

Figure 7. Ethyl 2-benzylidene acetoacetate versus time when the reaction was carried out in presence of 30-MLHM-NH_2 (●), 50-MLHM-NH_2 (■), 100-MLHM-NH_2 (▲) and 100-LHM-TEMS (◆) materials as catalysts at 80ºC, with 10 mol% of active sites in acetonitrile as solvent.

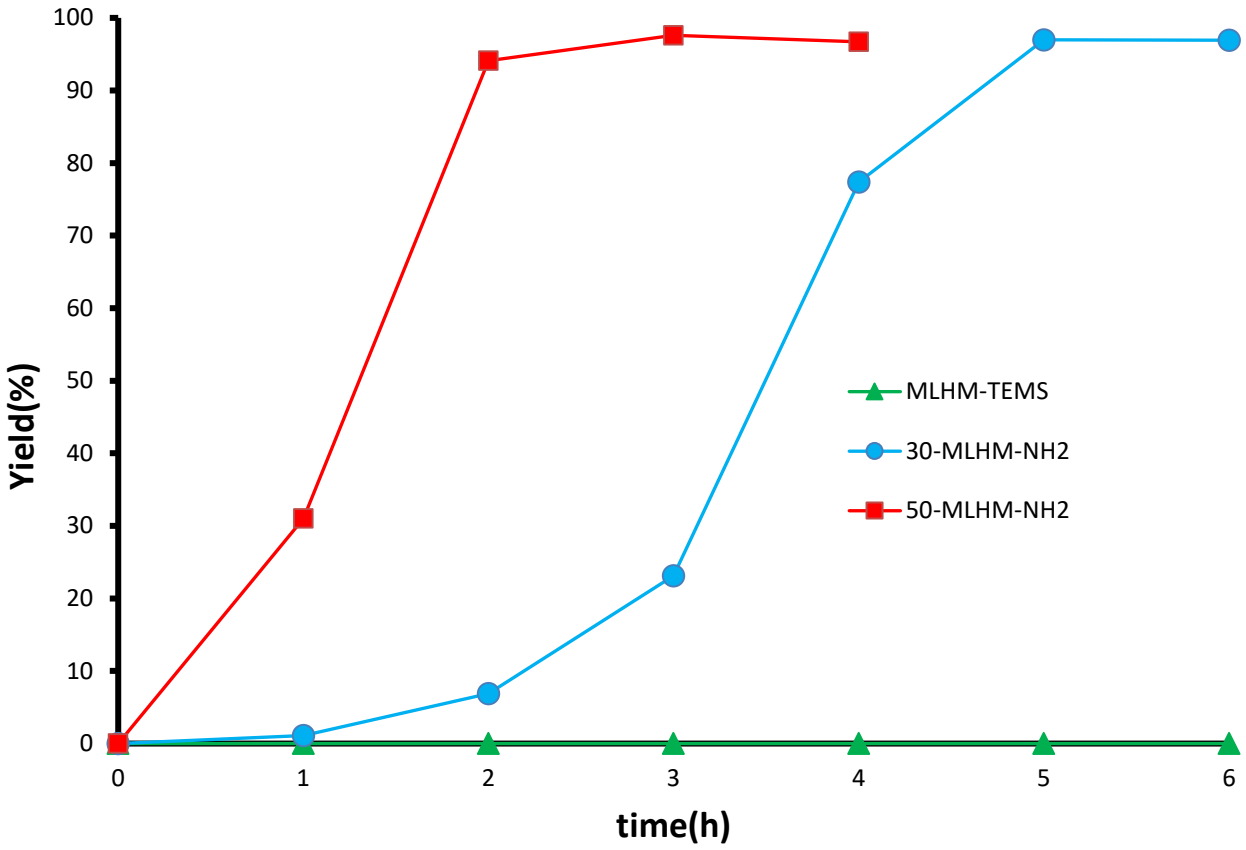

Figure 8. Nitrostyrene versus time when the reaction was carried out in presence of 30-MLHM-NH_2 (●), 50-MLHM-NH_2 (■) and 100-LHM-TEMS (◆) materials as catalysts at 90ºC, with 5 mol% of active sites in anisole as solvent.

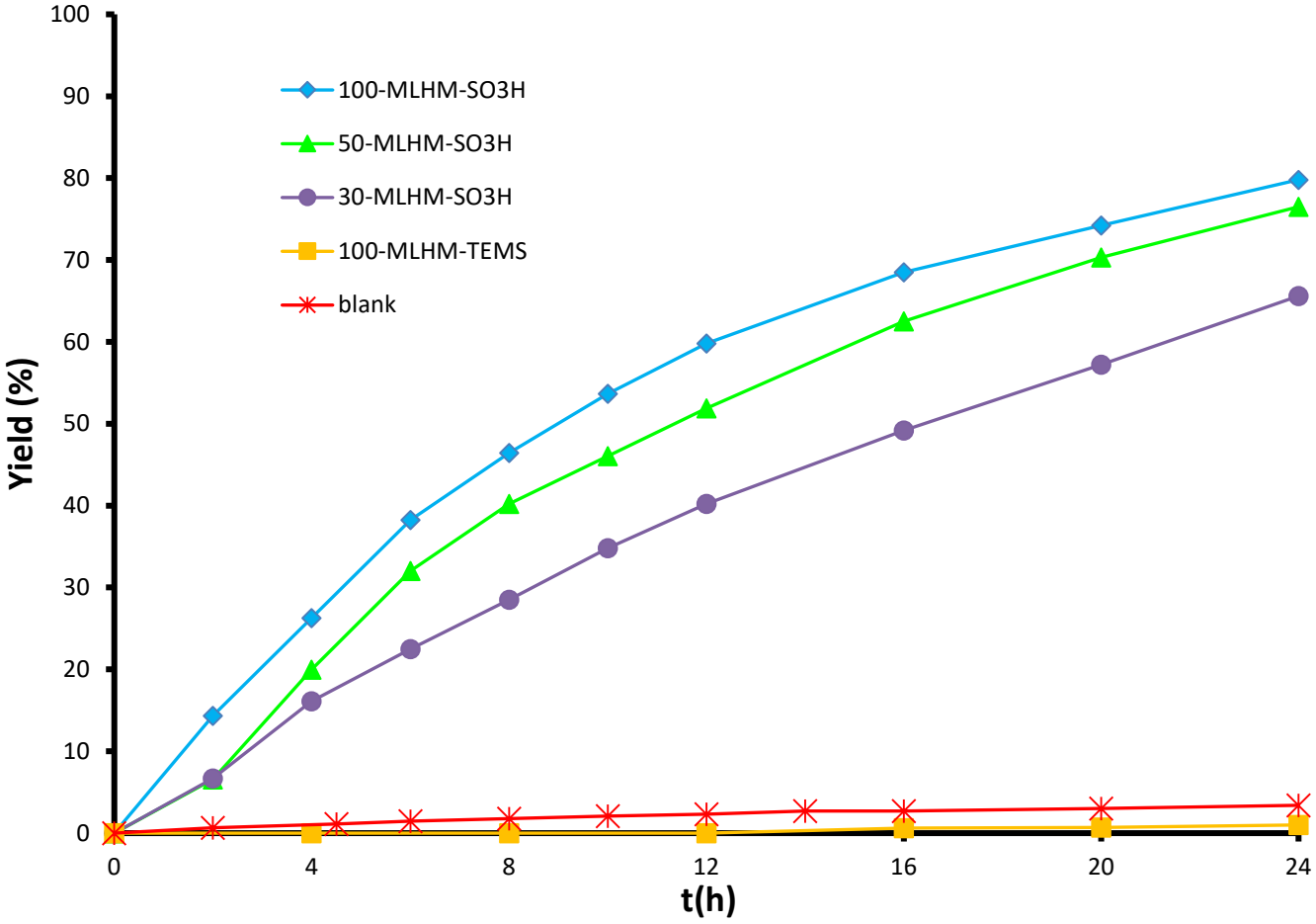

Figure 9. 1,1-dimethoxytoluene versus time when the reaction was carried out in presence of 100-MLHM-SO_3H (◆),50-MLHM-SO_3H (▲), 30-MLHM-SO_3H, (●) 100-LHM-TEMS (■) and blank (✱) at 45ºC and with 10% mol of active sites.

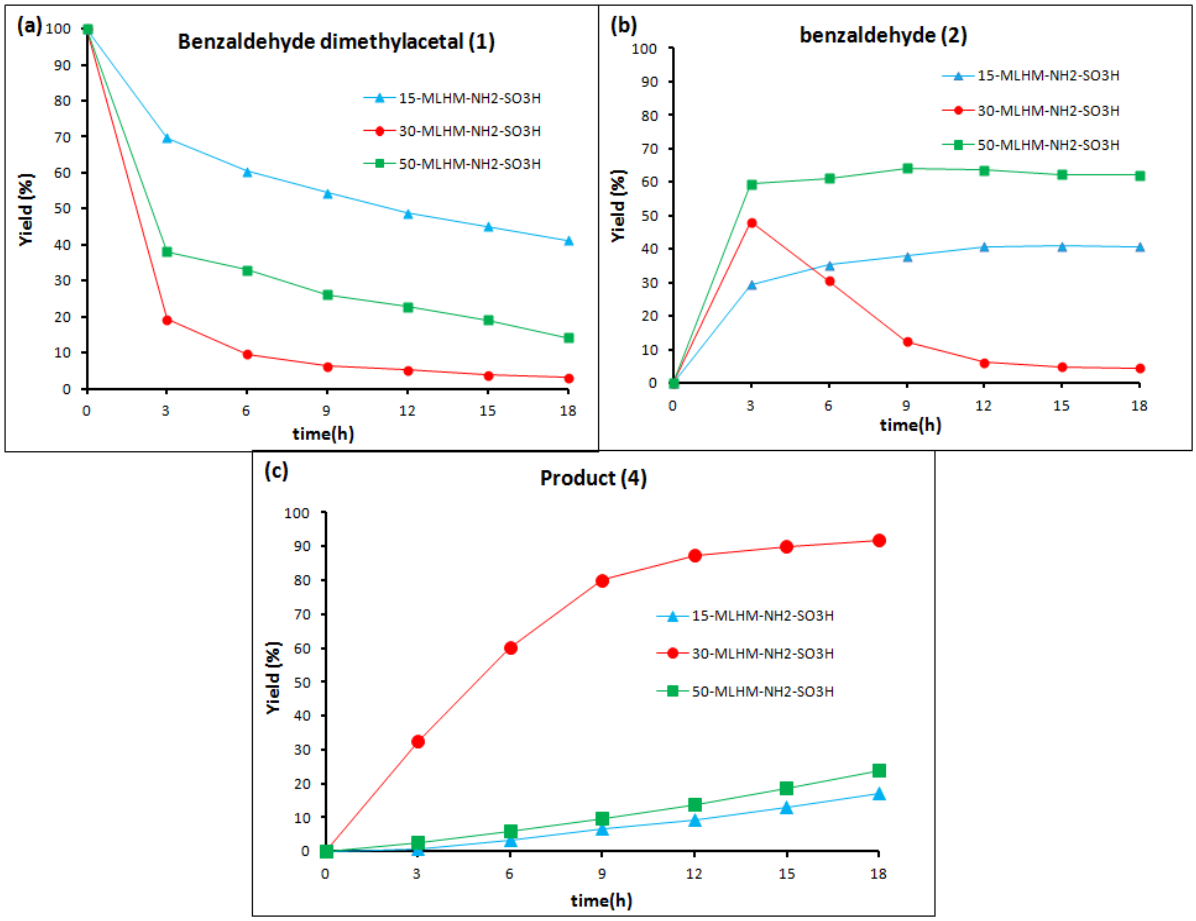

Figure 10. Catalytic activity in the one-pot acetal hydrolysis-Knoevenagel condensation of ethyl cyanoacetate carried out by bifunctional hybrids materials: 15-MLHM-NH_2-SO_3H (▲), 30-MLHM-NH_2-SO_3H (●) and 50-MLHM-NH_2-SO_3H (■). (a) Conversion of benzaldehyde dimethylacetate (1), (b) Yield of benzaldehyde (2), (c) Yield of final product (4).

References

(1) Ferey, G., Hybrid porous solids: past, present, future. *Chem. Soc. Rev.* **2008**, 37, 191-214.
(2) Loy, D. A.; Shea, K. J., Bridged Polysilsesquioxanes. Highly Porous Hybrid Organic-Inorganic Materials. *Chem. Rev. (Washington, D. C.)* **1995**, 95, 1431-42.
(3) Diaz, U.; Brunel, D.; Corma, A., Catalysis using multifunctional organosiliceous hybrid materials. *Chem. Soc. Rev.* **2013**, 42, 4083-4097.
(4) Rowsell, J. L. C.; Yaghi, O. M., Metal–organic frameworks: a new class of porous materials. *Microporous Mesoporous Mater.* **2004**, 73, 3-14.
(5) Cheetham, A. K.; Rao, C. N. R.; Feller, R. K., Structural diversity and chemical trends in hybrid inorganic-organic framework materials. *Chem. Commun. (Cambridge, U. K.)* **2006**, 4780-4795.
(6) González-Arellano, C.; Corma, A.; Iglesias, M.; Sánchez, F., Improved Palladium and Nickel Catalysts Heterogenised on Oxidic Supports (Silica, MCM-41, ITQ-2, ITQ-6). *Adv. Synth. Catal.* **2004**, 346, 1316-1328.
(7) Ajami, D.; Liu, L.; Rebek Jr, J., Soft templates in encapsulation complexes. *Chem. Soc. Rev.* **2015**, 44, 490-499.
(8) Morell, J.; Gungerich, M.; Wolter, G.; Jiao, J.; Hunger, M.; Klar, P. J.; Froba, M., Synthesis and characterization of highly ordered bifunctional aromatic periodic mesoporous organosilicas with different pore sizes. *J. Mater. Chem.* **2006**, 16, 2809-2818.
(9) Kuschel, A.; Drescher, M.; Kuschel, T.; Polarz, S., Bifunctional Mesoporous Organosilica Materials and Their Application in Catalysis: Cooperative Effects or Not? *Chem. Mater.* **2010**, 22, 1472-1482.
(10) Wight, A. P.; Davis, M. E., Design and Preparation of Organic−Inorganic Hybrid Catalysts. *Chem. Rev.* **2002**, 102, 3589-3614.
(11) Hoffmann, F.; Cornelius, M.; Morell, J.; Fröba, M., Silica-Based Mesoporous Organic–Inorganic Hybrid Materials. *Angew. Chem. Int. Ed.* **2006**, 45, 3216-3251.
(12) Yamamoto, K.; Sakata, Y.; Nohara, Y.; Takahashi, Y.; Tatsumi, T., Organic-Inorganic Hybrid Zeolites Containing Organic Frameworks. *Science* **2003**, 300, 470-472.
(13) Férey, G., The Simplicity of Complexity--Rational Design of Giant Pores. *Science* **2001**, 291, 994-995.
(14) Ding, S.-Y.; Wang, W., Covalent organic frameworks (COFs): from design to applications. *Chem. Soc. Rev.* **2013**, 42, 548-568.
(15) Garcia-Garcia, P.; Zagdoun, A.; Coperet, C.; Lesage, A.; Diaz, U.; Corma, A., In situ preparation of a multifunctional chiral hybrid organic-inorganic catalyst for asymmetric multicomponent reactions. *Chemical Science* **2013**, 4, 2006-2012.
(16) McDonald, A. R.; Mueller, C.; Vogt, D.; van Klink, G. P. M.; van Koten, G., BINAP-Ru and -Rh catalysts covalently immobilized on silica and their repeated application in asymmetric hydrogenation. *Green Chem.* **2008**, 10, 424-432.
(17) Fujita, S.; Inagaki, S., Self-Organization of Organosilica Solids with Molecular-Scale and Mesoscale Periodicities. *Chem. Mater.* **2008**, 20, 891-908.
(18) Corriu, R. J. P.; Moreau, J. J. E.; Thepot, P.; Man, M. W. C., New mixed organic-inorganic polymers: hydrolysis and polycondensation of bis(trimethoxysilyl)organometallic precursors. *Chem. Mater.* **1992**, 4, 1217-24.
(19) Inagaki, S.; Guan, S.; Ohsuna, T.; Terasaki, O., An ordered mesoporous organosilica hybrid material with a crystal-like wall structure. *Nature* **2002**, 416, 304-307.
(20) Cooper, E. R.; Andrews, C. D.; Wheatley, P. S.; Webb, P. B.; Wormald, P.; Morris, R. E., Ionic liquids and eutectic mixtures as solvent and template in synthesis of zeolite analogues. *Nature (London, U. K.)* **2004**, 430, 1012-1016.
(21) Jones, C. W.; Tsuji, K.; Davis, M. E., Organic-functionalized molecular sieves as shape-selective catalysts. *Nature* **1998**, 393, 52-54.
(22) Gascon, J.; Corma, A.; Kapteijn, F.; Llabres i. Xamena, F. X., Metal Organic Framework Catalysis: Quo vadis? *ACS Catal.* **2014**, 4, 361-378.

(23) Ayala, V.; Corma, A.; Iglesias, M.; Rincón, J. A.; Sánchez, F., Hybrid organic—inorganic catalysts: a cooperative effect between support, and palladium and nickel salen complexes on catalytic hydrogenation of imines. *J. Catal.* **2004**, 224, 170-177.
(24) Inagaki, S.; Guan, S.; Fukushima, Y.; Ohsuna, T.; Terasaki, O., Novel Mesoporous Materials with a Uniform Distribution of Organic Groups and Inorganic Oxide in Their Frameworks. *J. Am. Chem. Soc.* **1999**, 121, 9611-9614.
(25) Beaudoin, D.; Maris, T.; Wuest, J. D., Constructing monocrystalline covalent organic networks by polymerization. *Nat. Chem.* **2013**, 5, 830-834.
(26) Ruiz-Hitzky, E.; Darder, M.; Aranda, P., Functional biopolymer nanocomposites based on layered solids. *J. Mater. Chem.* **2005**, 15, 3650-3662.
(27) Roth, W. J.; Shvets, O. V.; Shamzhy, M.; Chlubna, P.; Kubu, M.; Nachtigall, P.; Cejka, J., Postsynthesis Transformation of Three-Dimensional Framework into a Lamellar Zeolite with Modifiable Architecture. *J. Am. Chem. Soc.* **2011**, 133, 6130-6133.
(28) Margelefsky, E. L.; Zeidan, R. K.; Davis, M. E., Cooperative catalysis by silica-supported organic functional groups. *Chem. Soc. Rev.* **2008**, 37, 1118-1126.
(29) Notestein, J. M.; Katz, A., Enhancing heterogeneous catalysis through cooperative hybrid organic-inorganic interfaces. *Chem. - Eur. J.* **2006**, 12, 3954-3965.
(30) Fuerte, A.; Iglesias, M.; Sánchez, F.; Corma, A., Chiral dioxomolybdenum(VI) and oxovanadium(V) complexes anchored on modified USY-zeolite and mesoporous MCM-41 as solid selective catalysts for oxidation of sulfides to sulfoxides or sulfones. *J. Mol. Catal. A: Chem.* **2004**, 211, 227-235.
(31) Corma, A.; Fornes, V.; Pergher, S. B.; Maesen, T. L. M.; Buglass, J. G., Delaminated zeolite precursors as selective acidic catalysts. *Nature* **1998**, 396, 353-356.
(32) Choi, M.; Na, K.; Kim, J.; Sakamoto, Y.; Terasaki, O.; Ryoo, R., Stable single-unit-cell nanosheets of zeolite MFI as active and long-lived catalysts. *Nature* **2009**, 461, 246-249.
(33) Jung, J.; Jo, C.; Cho, K.; Ryoo, R., Zeolite nanosheet of a single-pore thickness generated by a zeolite-structure-directing surfactant. *J. Mater. Chem.* **2012**, 22, 4637-4640.
(34) Bellussi, G.; Montanari, E.; Di Paola, E.; Millini, R.; Carati, A.; Rizzo, C.; O'Neil Parker, W.; Gemmi, M.; Mugnaioli, E.; Kolb, U.; Zanardi, S., ECS-3: A Crystalline Hybrid Organic–Inorganic Aluminosilicate with Open Porosity. *Angew. Chem. Int. Ed.* **2012**, 51, 666-669.
(35) Gaona, A.; Moreno, J. M.; Velty, A.; Diaz, U.; Corma, A., One-pot synthesis of hierarchical porous layered hybrid materials based on aluminosilicate sheets and organic functional pillars. *Journal of Materials Chemistry A* **2014**, 2, 19360-19375.
(36) Gregg, S. J.; Sing, K. S. W., *Adsorption, surface area, and porosity*. Academic Press: London; New York, 1982.
(37) Sing, K. S. W.; Everett, D. H.; Haul, R. A. W.; Moscou, L.; Pierotti, R. A.; Rouquerol, J.; Siemieniewska, T., Reporting physisorption data for gas/solid systems with special reference to the determination of surface area and porosity. *Pure Appl. Chem.* **1985**, 57, 603-619.
(38) Barrett, E. P.; Joyner, L. G.; Halenda, P. P., The Determination of Pore Volume and Area Distributions in Porous Substances. I. Computations from Nitrogen Isotherms. *Journal of the American Chemical Society* **1951**, 73, 373-380.
(39) Dailey, J. S.; Pinnavaia, T. J., Silica-pillared derivatives of H+-magadiite, a crystalline hydrated silica. *Chem. Mater.* **1992**, 4, 855-863.
(40) Brenn, U.; Ernst, H.; Freude, D.; Herrmann, R.; Jähnig, R.; Karge, H. G.; Kärger, J.; König, T.; Mädler, B.; Pingel, U. T.; Prochnow, D.; Schwieger, W., Synthesis and characterization of the layered sodium silicate ilerite. *Microporous Mesoporous Mater.* **2000**, 40, 43-52.
(41) Fletcher, R.; Bibby, D., Synthesis of kenyaite and magadiite in the presence of various anions. *Clays Clay Miner.* **1987**, 35, 318.
(42) Mochizuki, D.; Shimojima, A.; Imagawa, T.; Kuroda, K., Molecular Manipulation of Two- and Three-Dimensional Silica Nanostructures by Alkoxysilylation of a Layered Silicate Octosilicate and Subsequent Hydrolysis of Alkoxy Groups. *Journal of the American Chemical Society* **2005**, 127, 7183-7191.

(43) Blake, A. J.; Franklin, K. R.; Lowe, B. M., Preparation and properties of piperazine silicate (EU-19) and a silica polymorph (EU-20). *J. Chem. Soc., Dalton Trans.* **1988**, 2513-2517.
(44) Bellussi, G.; Carati, A.; Di Paola, E.; Millini, R.; Parker Jr, W. O. N.; Rizzo, C.; Zanardi, S., Crystalline hybrid organic–inorganic alumino-silicates. *Microporous Mesoporous Mater.* **2008**, 113, 252-260.
(45) Wang, Q.; Gao, Y.; Luo, J.; Zhong, Z.; Borgna, A.; Guo, Z.; O'Hare, D., Synthesis of nano-sized spherical Mg3Al-CO3 layered double hydroxide as a high-temperature CO2 adsorbent. *RSC Advances* **2013**, 3, 3414-3420.
(46) Schreyeck, L.; Caullet, P.; Mougenel, J.-C.; Guth, J.-L.; Marler, B., A layered microporous aluminosilicate precursor of FER-type zeolite. *J. Chem. Soc., Chem. Commun.* **1995**, 2187-2188.
(47) Rodriguez, I.; Iborra, S.; Rey, F.; Corma, A., Heterogeneized Brönsted base catalysts for fine chemicals production: grafted quaternary organic ammonium hydroxides as catalyst for the production of chromenes and coumarins. *Applied Catalysis A: General* **2000**, 194–195, 241-252.
(48) Climent, M. J.; Corma, A.; Iborra, S.; Epping, K.; Velty, A., Increasing the basicity and catalytic activity of hydrotalcites by different synthesis procedures. *J. Catal.* **2004**, 225, 316-326.
(49) Prout, F. S.; Beaucaire, V. D.; Dyrkacz, G. R.; Koppes, W. M.; Kuznicki, R. E.; Marlewski, T. A.; Pienkowski, J. J.; Puda, J. M., Konevenagel Reaction. Kinetic study of the reaction of (+)-3-methyl-cyclohexanone with malononitrile. *The Journal of Organic Chemistry* **1973**, 38, 1512-1517.
(50) Jones, G., The Knoevenagel condensation. *Organic reactions* **1967**, 15, 204-599.
(51) Guyot, J.; Kergomard, A., Cinétique et mécanisme de la réaction de knoevenagel dans le benzène-2. *Tetrahedron* **1983**, 39, 1167-1179.
(52) Lubisch, W.; Beckenbach, E.; Bopp, S.; Hofmann, H.-P.; Kartal, A.; Kästel, C.; Lindner, T.; Metz-Garrecht, M.; Reeb, J.; Regner, F.; Vierling, M.; Möller, A., Benzoylalanine-Derived Ketoamides Carrying Vinylbenzyl Amino Residues: Discovery of Potent Water-Soluble Calpain Inhibitors with Oral Bioavailability. *J. Med. Chem.* **2003**, 46, 2404-2412.
(53) Vlok, N.; Malan, S. F.; Castagnoli, N.; Bergh, J. J.; Petzer, J. P., Inhibition of monoamine oxidase B by analogues of the adenosine A2A receptor antagonist (E)-8-(3-chlorostyryl)caffeine (CSC). *Biorg. Med. Chem.* **2006**, 14, 3512-3521.
(54) Selvam, C.; Jachak, S. M.; Thilagavathi, R.; Chakraborti, A. K., Design, synthesis, biological evaluation and molecular docking of curcumin analogues as antioxidant, cyclooxygenase inhibitory and anti-inflammatory agents. *Bioorg. Med. Chem. Lett.* **2005**, 15, 1793-1797.
(55) Nakayama, K.; Ishida, Y.; Ohtsuka, M.; Kawato, H.; Yoshida, K.-i.; Yokomizo, Y.; Hosono, S.; Ohta, T.; Hoshino, K.; Ishida, H.; Yoshida, K.; Renau, T. E.; Léger, R.; Zhang, J. Z.; Lee, V. J.; Watkins, W. J., MexAB-OprM-Specific efflux pump inhibitors in Pseudomonas aeruginosa. Part 1: Discovery and early strategies for lead optimization. *Bioorg. Med. Chem. Lett.* **2003**, 13, 4201-4204.
(56) Rodriguez, I.; Sastre, G.; Corma, A.; Iborra, S., Catalytic Activity of Proton Sponge: Application to Knoevenagel Condensation Reactions. *J. Catal.* **1999**, 183, 14-23.
(57) Beaumont, R.; Barthomeuf, D., X, Y, aluminum-deficient and ultrastable faujasite-type zeolites. II. Acid strength and aluminum site reactivity. *J. Catal.* **1972**, 27, 45-51.
(58) Pine, L. A.; Maher, P. J.; Wachter, W. A., Prediction of cracking catalyst behavior by a zeolite unit cell size model. *J. Catal.* **1984**, 85, 466-476.
(59) Gianotti, E.; Diaz, U.; Velty, A.; Corma, A., Strong Organic Bases as Building Blocks of Mesoporous Hybrid Catalysts for C–C Forming Bond Reactions. *Eur. J. Inorg. Chem.* **2012**, 2012, 5175-5185.
(60) Luzzio, F. A., The Henry reaction: recent examples. *Tetrahedron* **2001**, 57, 915-945.
(61) Sartori, G.; Bigi, F.; Maggi, R.; Sartorio, R.; Macquarrie, D. J.; Lenarda, M.; Storaro, L.; Coluccia, S.; Martra, G., Catalytic activity of aminopropyl xerogels in the selective synthesis of (E)-nitrostyrenes from nitroalkanes and aromatic aldehydes. *J. Catal.* **2004**, 222, 410-418.
(62) Climent, M. J.; Corma, A.; Iborra, S., Heterogeneous Catalysts for the One-Pot Synthesis of Chemicals and Fine Chemicals. *Chem. Rev.* **2011**, 111, 1072-1133.

(63) Hara, T.; Kanai, S.; Mori, K.; Mizugaki, T.; Ebitani, K.; Jitsukawa, K.; Kaneda, K., Highly Efficient C−C Bond-Forming Reactions in Aqueous Media Catalyzed by Monomeric Vanadate Species in an Apatite Framework. *The Journal of Organic Chemistry* **2006**, 71, 7455-7462.
(64) Poe, S. L.; Kobašlija, M.; McQuade, D. T., Microcapsule Enabled Multicatalyst System. *Journal of the American Chemical Society* **2006**, 128, 15586-15587.
(65) Greene, T. W.; Wuts, P. G. M., *Protective Groups in Organic Synthesis. 2nd Ed*. John Wiley and Sons, Inc.: 1991; p 473 pp.
(66) Hanessian, S.; Editor, *Preparative Carbohydrate Chemistry*. Dekker: 1997; p 648 pp.
(67) Li, T.-S.; Li, S.-H.; Li, J.-T.; Li, H.-Z., Montmorillonite Clay Catalysis. Part 2.1 An Efficient and Convenient Procedure for the Preparation of Acetals catalysed by Montmorillonite K-10. *J. Chem. Res., Synop.* **1997**, 26-27.
(68) Matysiak, S.; Frank, R.; Pfleiderer, W., Acetal Oligonucleotide Conjugates in Antisense Strategy. *Nucleosides and Nucleotides* **1997**, 16, 855-861.
(69) Ashton, M. J.; Lawrence, C.; Karlsson, J.-A.; Stuttle, K. A. J.; Newton, C. G.; Vacher, B. Y. J.; Webber, S.; Withnall, M. J., Anti-inflammatory 17β-Thioalkyl-16α,17α-ketal and -acetal Androstanes: A New Class of Airway Selective Steroids for the Treatment of Asthma. *J. Med. Chem.* **1996**, 39, 4888-4896.
(70) Bauer, K.; Garbe, D.; Surburg, H. Natural Raw Materials in the Flavor and Fragrance Industry. In *Common Fragrance and Flavor Materials*; Wiley-VCH Verlag GmbH: 2001, pp 167-226.
(71) Tanabe, K.; Hölderich, W. F., Industrial application of solid acid–base catalysts. *Applied Catalysis A: General* **1999**, 181, 399-434.
(72) Garczarek, F.; Gerwert, K., Functional waters in intraprotein proton transfer monitored by FTIR difference spectroscopy. *Nature (London, U. K.)* **2006**, 439, 109-112.
(73) Gianotti, E.; Diaz, U.; Velty, A.; Corma, A., Designing bifunctional acid–base mesoporous hybrid catalysts for cascade reactions. *Catalysis Science & Technology* **2013**, 3, 2677-2688.

TOC